AD-A126 060 AN EXPERIMENTAL STUDY OF A HIGH ROTATIONAL SPEED PROPULSOR(U) LEHMAN (A F) ASSOCIATES INC CENTERPORT NY A F LEHMAN ET AL. JAN 83 USNA-EW-01-83 1/1

UNCLASSIFIED F/G 21/5 NL

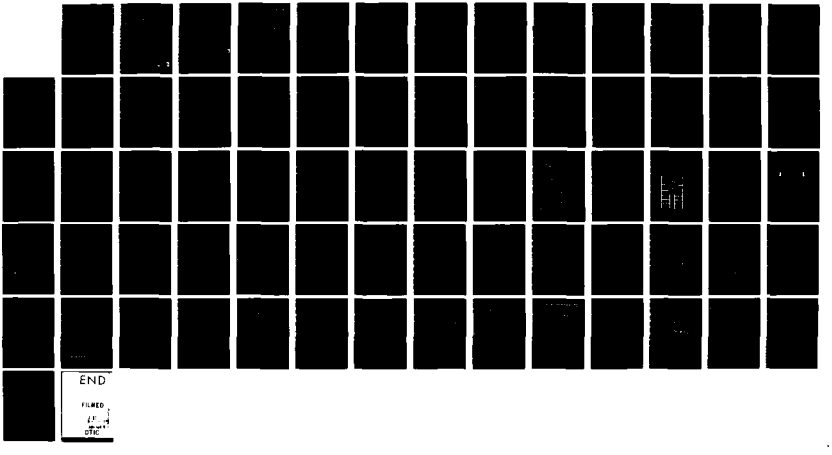

END

FILMED

DTIC

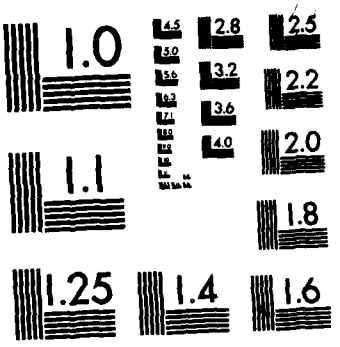

MICROCOPY RESOLUTION TEST CHART
NATIONAL BUREAU OF STANDARDS-1963-A

AD A126060

DTIC FILE COPY

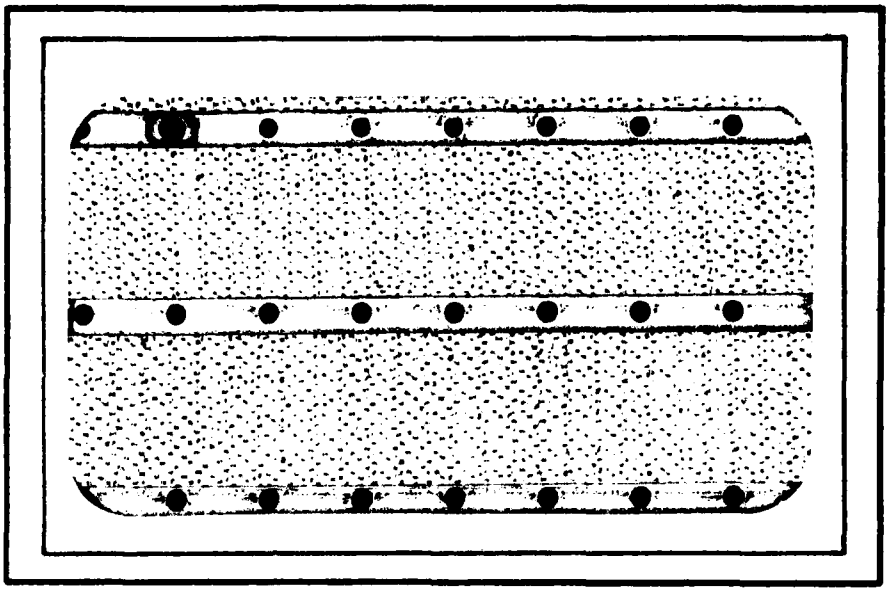

UNITED STATES NAVAL ACADEMY
DIVISION OF
ENGINEERING AND WEAPONS
ANNAPOLIS, MARYLAND

United States Naval Academy
Annapolis, Maryland 21402

Division of Engineering and Weapons
Hydromechanics Laboratory

Report EW-01-83

An Experimental Study of a High Rotational Speed Propulsor

by

August F. Lehman
A.F. Lehman Associates Incorporated

John Hill
U.S. Naval Academy

January 1983

UNCLASSIFIED

SECURITY CLASSIFICATION OF THIS PAGE (When Data Entered)

REPORT DOCUMENTATION PAGE		READ INSTRUCTIONS BEFORE COMPLETING FORM
1. REPORT NUMBER EW-01-83	2. GOVT ACCESSION NO. AD-A126 068	3. RECIPIENT'S CATALOG NUMBER
4. TITLE (and Subtitle) An Experimental Study of a High Rotational Speed Propulsor		5. TYPE OF REPORT & PERIOD COVERED Technical 6. PERFORMING ORG. REPORT NUMBER
7. AUTHOR(s) August F. Lehman John Hill		8. CONTRACT OR GRANT NUMBER(s)
9. PERFORMING ORGANIZATION NAME AND ADDRESS Hydromechanics Laboratory U.S. Naval Academy Annapolis, MD 21402		10. PROGRAM ELEMENT, PROJECT, TASK AREA & WORK UNIT NUMBERS N0002482WR13030
11. CONTROLLING OFFICE NAME AND ADDRESS Naval Sea Systems Command Washington, D.C.		12. REPORT DATE January 1983 13. NUMBER OF PAGES 66
14. MONITORING AGENCY NAME & ADDRESS(if different from Controlling Office)		15. SECURITY CLASS. (of this report) UNCLAS 15a. DECLASSIFICATION/DOWNGRADING SCHEDULE

16. DISTRIBUTION STATEMENT (of this Report)

Distribution Unlimited

17. DISTRIBUTION STATEMENT (of the abstract entered in Block 20, if different from Report)

18. SUPPLEMENTARY NOTES

19. KEY WORDS (Continue on reverse side if necessary and identify by block number)

Propulsor, Ultra-High Speed, Helix Vane System

20. ABSTRACT (Continue on reverse side if necessary and identify by block number)

A study of an ultra-high rotational speed propulsor, including experimental results, is detailed. The propulsor consists of a helix vane system encapsulated by a thin shell, with a fixed shroud at the exit to convert the radial and rotational velocity components into an axial velocity. The necessity of including the velocity wake deficit of the propulsor (itself) in the design considerations is described.

DD FORM 1 JAN 73 1473 EDITION OF 1 NOV 65 IS OBSOLETE
S/N 0102-014-6601

UNCLASSIFIED

SECURITY CLASSIFICATION OF THIS PAGE (When Data Entered)

AN EXPERIMENTAL STUDY OF A HIGH ROTATIONAL SPEED PROPULSOR

BY

August F. Lehman
A. F. Lehman Associates Incorporated, Centerport, New York

AND

John Hill
U.S. Naval Academy

TABLE OF CONTENTS

TABLE OF CONTENTS (Continued)

ABSTRACT

This report discusses an initial study of an ultra-high rotational speed propulsor. The propulsor consists of a helix vane system encapsulated by a thin shell. A fixed shroud at the exit converts the radial and rotational velocity components into axial velocity and/or pressure head gains — both of which produce thrust. The ultra-high rotational speed should allow direct coupling to a turbine thus permitting higher horsepowers in less spatial volume. The low pressure region developed inside the propulsor can be used as a "sink" for open cycle gas exhaust turbines (thereby reducing the depth dependent back pressure operational penalty) or as a source for afterbody boundary layer control. Power demand relationships have been (tentatively) identified for the exterior surface frictional drag of the shell, the transfer of rotational velocity from the propulsor to the liquid passing through and the magnitude of the low pressure region. A notable difference between the thrust producing design considerations of this concept and those of propellers and pumpjets lies in the necessity of including the velocity wake deficit of the propulsor (itself) in establishing the flow rate and momentum change required for specific thrusts.

NOMENCLATURE

A	=	Area (ft^2)
C_f	=	Drag coefficient (from Reference 2)
D	=	Drag (lbs)
F	=	Force (lbs)
g	=	Gravity (ft/sec^2)
H	=	Hydraulic head ($V^2/2g$)
hp	=	Horsepower (ft-lb/sec)
J	=	Advance Ratio
J_M	=	Moment of inertia about the axis of rotation ($ft\text{-}lb/sec^2$)
K_Q	=	Torque Coefficient
K_T	=	Thrust Coefficient
M	=	Mass (slugs)
n	=	Rotational Speed (rps)
p	=	Pressure (psf)
Δp	=	Difference in pressure (psf)
Q	=	Flow Rate (cfs)
r	=	Radius (ft)
T	=	Torque (lb-ft)
T_o	=	Unbalanced torque (lb-ft)
V	=	Velocity (fps)
w_t	=	Tangential induced velocity (fps)
x	=	Axial or radial distance (ft)
y	=	Height of fluid (ft) above the vertex defined in Equation 1
α	=	Angular acceleration (rad/sec^2)
γ	=	Specific weight (lb/ft^3)
η	=	Efficiency
κ	=	Goldstein's Kappa Function
ρ	=	Mass density (slugs)
ν	=	Kinematic viscosity (ft^3/sec^2)
ω	=	Angular velocity (rad/sec)

INTRODUCTION

When considering (a) the broad range of propulsor requirements for underwater weapons and (b) the technology existing in high rotational speed turbines, it appears that certain propulsor system operational advantages might be gained by having a propulsor which could be directly coupled to a high rotational speed turbine. The advantage of employing a high rotational speed turbine without a gear reducer lies in the fact that as the rotational speed increases, more horsepower can be packaged in the same spacial volume. The propulsor concept examined in this study was proposed because it offered the possibility of improved performance over the following types:

1. supercavitating or ventilated propellers (which do offer the advantage of high rotational speeds),

2. underwater gas exhaust rockets (which have relatively low propulsive efficiencies) and,

3. propulsors driven by open cycle turbines having their gas exhaust via a hollow propulsor drive shaft (where the depth of submergence, i.e, the back pressure on the turbine has a pronounced effect on turbine efficiency).

Furthermore, the propulsor should be relatively inexpensive as a simple investment casting should be an acceptable method of production.

CONCEPTIONAL BACKGROUND

While the long range goal of this concept envisions a high rotational speed turbine with the propulsor forming the central section of the turbine, i.e., the turbine is "wrapped around" the propulsor as shown in Figure 1, the present study focuses on the propulsor itself. The basic objective of the present study was to gather experimental data so as to gain an insight into some of the hydrodynamic performance characteristics of the concept which could then be utilized in the further development of propulsors of this type. Of course, in order to gain the desired information, a "Basic Propulsor" had to be designed to serve as a test bed.

Simply put, the propulsor concept consists of an ultra-high rotational speed helix vane system which is enclosed by a cylindrical shell. The intake or forward portion of the propulsor will be referred to as the "inducer" region of the propulsor in the subsequent discussions. The aft portion of the propulsor will be referred to as the "pump" region. In the Basic Propulsor, the "inducer" consists of a constant pitch helix vane system

while the "pump" consists of a vane system having an ever increasing pitch. This arrangement is shown in Figure 2.

The Basic Propulsor concept rests upon the following:

1. inducer design as employed in liquid rocket engine turbopumps,

2. the change in momentum as introduced via an accelerated mass and,

3. the effect of rotation upon a liquid contained in a vessel.

Inducer Region

In a turbopump, the inducer is located in the axial inlet portion of the pump. Its purpose is to raise the inlet head sufficiently high to prevent (or at least minimize) the loss of efficiency as a result of subsequent cavitation in the pump. Consequently, in rocket engine application, the inducer is designed to produce high suction performance. In an underwater weapon propulsion application, compatible high suction performance requirements are not needed since operation of a vehicle 50 feet or more below the surface of the ocean results in total inlet head pressures (above vapor pressure) so high as to place essentially no restriction on the inducer design. Consequently, the inducer portion of this propulsor concept was envisioned solely as a means of ingesting water and presenting it to the pump portion during a launch or swim-out stage. Once the forward design velocity of the vehicle is attained, the inducer adds no axial velocity to the flow although it will impart rotational velocity to the confined flow-through stream.

Pump Region

The aft (pump) region of the propulsor develops the desired thrust. It does this by introducing a continuously increasing axial flow component from the start to the exit of the pump portion of the propulsor via the change in the vane helix pitch and, because the flow rate is constant, the cross-sectional area of the flow at any axial station in the pump portion of the propulsor is reduced. This reduction in the flow area which is occurring inside a fixed cross-sectional area shell will create a central low pressure or void region which will be discussed in the following section.

Rotation Effects

The high rotational speed of the propulsor brings into play one of the factors mentioned earlier, i.e., that of the effect of rotation upon a confined liquid. If a vessel is filled with a liquid and is rotated about a central vertical axis, the liquid will (eventually) acquire the angular velocity of the vessel. If the vessel is partially filled, the free surface will form a parabola of the form:

$$y = \frac{\omega^2 x^2}{2g} \qquad \text{Equation (1)}$$

where y is the distance above the liquid surface existing at the axis of rotation, x is the radial distance from the axis of rotation to the surface of the liquid at y and g is the gravitional force. It follows then that y is the pressure head (i.e., in feet of liquid) over that existing at the liquid surface at the axis of rotation. Consequently, if an open vessel is filled to the top with water and then rotated abou a central vertical axis, water will spill over the top edge and, if openings are placed in the bottom of the vessel, water will continue to enter at the bottom and spill over the top. From this it can be seen that any rotational velocity introduced to the liquid as it passes through the propulsor will contribute to the "pump" performance of the propulsor — but, perhaps, equally important, when considering the application of this concept to an underwater weapon, is the fact that the centrifugal component of the flow increases the local static head on the vane system in the "pump" region and this, in turn, will reduce cavitation susceptibility. In the proposed concept it is expected this result will be accomplished in the following manner.

It has already been mentioned that the propulsor can be described as a "shell surrounded" helix vane system or as a helix vane system attached to a rotating shroud. Next, it has been pointed out that the cross-sectional area of the liquid in the pump portion is being continuously reduced since the ever increasing helix angle of the vanes increases the local axial velocity. Furthermore, the rotation of the confined liquid forces it to the walls of the shell. Thus, in this concept, it becomes possible to remove a central "core" portion of the hub and vanes (in the pump portion of the propulsor) since there should be no flow in that region. Furthermore, by limiting the vane height, i.e., the inward projection distance from the shell wall, to a value less than the "blanket thickness" of the flowing liquid at any given axial location, and remembering that the local static head will increase according to Equation (1), cavitation free performance should result provided sufficient rotational velocity is acquired by the flow.

The lower pressure region, resulting from the rotational and accelerating axial flows will create a high base drag unless this reduced pressure is minimized. There are several ways in which this could be

done. One way would be to utilize this region as an exhaust "sink" for an open cycle turbine exhaust thus improving turbine efficiency. Another way would be to bleed fluid surrounding the vehicle afterbody into this lower pressure region via a hollow drive shaft joining openings on the vehicle afterbody. This latter approach could introduce some boundary layer control. In any event, it is believed that the existence of this lower pressure region can be utilized to an advantage in the proposed concept. In the present study it was planned to permit air to bleed into the lower pressure region via a hollow drive shaft connected to a line above the water-line. The conceptual water flow path and the lower pressure region in the propulsor are shown in Figure 3.

OBJECTIVES

General

The basic objective of this study was to gather basic performance data which could be used in developing design guidelines and/or estimating the potential performance of the propulsor concept.

Specific

As mentioned earlier, the general informational guidelines used in the design of the propulsor shown in Figure 2 came from data on liquid rocket turbopump inducers and fundamental relationships involving liquids in motion. However, specific information about many of the hydrodynamic considerations which would affect performance is not available. In particular, hard data about the following was needed and was addressed in this study.

1. The frictional drag of the outer surface of a high rotational speed shell.

2. The transfer of rotational velocity to a liquid as it moves through a high rotational speed propulsor of the concept described.

3. The magnitude of the low pressure region created in the propulsor as a result of high rotational speeds and locally accelerating flows.

4. The ability of a fixed external shroud to convert the rotational and radial components of the exiting jet into axial components and/or gains in static pressure.

TEST FACILITIES

All tests were performed at the U.S. Naval Academy (USNA). It was originally planned to perform the tests in the 128 Meter High Performance Towing Tank. A towing tank rather than the more usually employed water tunnel was proposed for these propulsor tests because the planned bleeding of air into the lower pressure region would quickly saturate the flow in a water tunnel with air bubbles, i.e., the estimated quantity of air entering the flow stream was far in excess of that which can be removed by the usual degasing process. In a towing tank, the air bubbles would rise to the surface and exit into the atmosphere (before the next run) thereby creating no problem.

Testing was started in the towing tank and the propulsor was observed by the principal author riding on the carriage during carriage runs and by both authors during static or bollard conditions. It became apparent that the desired detail observation of the flow was not possible under forward velocity conditions simply because the time frame was too short. Consequently, after discussing the situation with Dr. Bruce Johnson,* it was decided to introduce some modifications to the propulsor (based on the then completed observations) and to continue testing in the USNA Circulating Water Channel since this facility would permit the longer observation times desired. Consequently, nearly all of the date reported here was obtained in the circulating water channel and only a few towing tank test results are shown to indicate agreement of the data obtained in the two different facilities.

The test section of the water channel is 1.31-ft (0.4 m) wide, 1.31-ft (0.4 m) deep and 5.05-ft (1.54 m) long. The maximum velocity is 26 fps (8 m/s), well in excess of the desired maximum for these tests of about 15 fps (4.6 m/s). The blockage presented by the test rig was considered acceptable in this study. Detailed descriptions of the towing tank and circulating water channel are presented in Reference 1.

TEST EQUIPMENT

The practical application of the proposed propulsor concept is based upon performance at ultra-high rotational speeds, say of the order of 30 - 50,000 rpm., i.e., with the propulsor directly coupled to a turbine. However, finding a prime mover possessing that rotational speed in a size

---

* Director, Hydromechanics Laboratory, USNA

suitable for test purposes in an exploratory program of this type was a bit difficult considering cost limitations and the fact the unit had to operate with the powering capabilities in existence at the test facility. Consequently, powering choices were limited to either off-the-shelf high speed electric motors or air turbines. It had been hoped to find a prime mover of the order of 15 hp — but that desire was rather quickly scaled down as vendor information became available. Air turbines had the advantage of high rotational speeds (and power outputs) in the range desired. But they also had two serious drawbacks. While one was their high cost, the major one concerned the method of supplying the necessary high pressure air or gas. The use of tanks of nitrogen was possible, but the total cost, i.e., a turbine plus an "air" supply became a bit much for this program. Consequently, what was selected was a pair of universal electric motors each having the capability of developing 2 hp at 12,000 rpm and having a permissible short time overload to about 2.5 hp but with an accompanying decrease in rotational speed. By coupling the two motors to a "T" gear box (two input shafts, one output shaft), there was available the order of 5 hp as propulsor input power. It was recognized that this relatively low horsepower placed somewhat severe restrictions on the range of operating conditions but it was believed that sufficient information could be acquired to satisfy the program objectives.

The basic test rig consisted of a Mercury Marine 20 hp racing unit with the engine replaced by the just mentioned twin electric motors. The lower end of the racing unit has a maximum diameter of 2-inches with the gearing capable of at least 15,000 rpm, consequently, it was excellent as an off-the-shelf component. The entire rig was supported so that a strain-gaged flexure block type of balance measured the axial force. The rotational speed was determined by having an electromagnetic pickup count pulses (2 pulses per shaft revolution) with the output in 2 x rps read on a digital volt meter.

Propulsor Configurations

The basic propulsor was introduced in the Conceptual Background Section and shown in Figure 2. However, as noted in the section on Specific Objectives, considerable fundamental information was desired and, therefore, other configurations were tested to acquire this data. These configurations will now be presented and serve as a guide when the test results are presented.

When the performance of a propulsor is discussed, configurations other than the Basic Propulsor (Figure 2) will be identified as to three major variables:

1. the forward part of the propulsor, i.e., the inducer
2. the aft part of the propulsor, i.e., the pump and,

3. the external shroud if one is employed.

Figure 4 shows an arrangement which permits a change in the aft or pump of the propulsor. Since the acquiring of rotational velocity by the flow through stream is of interest, changes in that variable could be noted by introducing "bars" on the interior of the smooth aft shell. The bars, of course, help the water adjacent to the interior wall acquire more of the shell rotational velocity than is possible with a smooth surface. As a last test, the aft portion was cut off thereby permitting a test of the constant helix angle inducer as a separate item.

Figure 5 shows the Basic Propulsor with the shroud while Figure 6 shows the inducer (only) with the "long tube" shroud. The shrouds could be run with or without honeycomb elements at the exit end. The honeycomb elements were employed to assist the shroud in the conversion of rotational flow into axial flow or gains in static head.

TEST PROCEDURES

The axial force calibration was determined through the application of dead weights on the propulsor centerline. A procedure was established for checking the calibration (again with dead weights) without removing the test rig from the channel. The calibration was checked before and at the conclusion of each day's runs. The calibration remained constant throughout the entire program.

The rotational speed acquisition system was checked by introducing a square wave of known frequencies to the system and spot checked with a strobe light during testing as observations of the propulsor were made.

The water velocity was obtained from the water channel's velocity meter, i.e., the nozzle pressure drop reading. That data could then be corrected using pitot tube velocity survey data acquired in the horizontal plane of the propulsor shaft. Surveys were made at both the leading edge of the propulsor and 1/2-inch behind the trailing edge of the shroud. This velocity comparison is shown in Figure 7. As might be expected, the pitot tube surveys indicate a higher velocity because of blockage.

Power to the motors was controlled by a 50 amp General Radio Variac. The power output from the variac was read directly on a Yokogawa Model 2433 Power Meter. This unit automatically takes into consideration the power factor thus the power reading was a true reading of the power going into the motors. No correction was made for the electric motor efficiency which may well change under different loading conditions. Consequently, the actual power values going to the drive

would be lower by whatever loss existed in the motors. However, for the purpose of these tests, i.e., the drawing of generalized conclusions, not considering the electric motor efficiency in the calculations was not considered crucial.

DATA PRESENTATION AND DISCUSSION

The tare data will be presented first with the presentation and discussion of the test results as it applies to the propulsor concept following.

Tare Drag of the Test Rig

The drag of the unit without the propulsor or shroud is shown in Figure 8. Three curves are shown. One curve (with data points) is that obtained in the water channel using the channel speed meter reading as the velocity. A second curve is that data corrected for channel blockage using pitot tube data. What that correction does is shift the data at a given velocity to a higher velocity. The third curve is from data obtained during the initial towing tank runs where the model was run at a slightly deeper depth of submergence. The "knee" in the water channel curve is believed due to the wave form and spray which were significant between 9 and 10 knots.

Frictional Power (kw) Demand of a High Rotational Speed Cylinder

In establishing the basic design an estimate of the power required to overcome the frictional resistance developed by the high rotational speed of the shell was made through the use of the flat plate drag equation:

$$D = C_f \ell \frac{\rho}{2} V^2 \qquad \text{Equation (2)}$$

where C_f* is a function of Reynolds number ($R_e = V\ell/\nu$). Values of C_f were obtained from the frictional drag coefficient curves of Reference 2. In calculating the drag and Reynolds number, ℓ is the flow path distance and V is the flow path velocity. Initial calculations of the power (kw) were made using the circumference as ℓ and the rotational velocity as V. The horsepower was derived from hp = Drag x Velocity/550. A plot of those values in terms of kw (which was the measured power quantity) is shown as one curve on Figure 9. Also shown is a curve of the calculated power with the introduction of a forward velocity of 9.3 fps. For this case, ℓ is the flow path along the shell and V is the vector magnitude

* C_f is defined for a plate of unit width.

of the axial and rotational velocity. It is to be expected that the calculated drag would increase enormously for this case as not only is ℓ becoming much larger than for the bollard case where it was a constant, i.e., the circumference, but the velocity also becomes larger. While C_f is becoming smaller as R_e increases, it cannot compensate for the huge increase in ℓ, i.e., at 100 rps ℓ is over six times the circumferential measurement.

Experimental data was obtained from two different types of tests. The first test series measured the power (kw) required to rotate a solid cylinder having the same external dimensions as the Basic Propulsor. This power can therefore be related to the frictional forces existing on the exterior surface and ends of the "dummy" propulsor. A second series of tests were run with a thin disk having the same outside diameter as the propulsor. The disk data was assumed to provide the "end(s)" effect on the power requirement of the complete cylinder or "dummy" propulsor. Consequently, the difference in power between the two sets of data is taken as that associated with the frictional drag of only the exterior of the rotating shell. Figure 10 shows the power demand of the "dummy" propulsor. Measurements were taken "in water" and "in air." Figure 11 shows the power demand of the thin disk. On this figure the difference between the two curves is taken as the power associated with just the disk and is taken as the "end effect" power to be subtracted from the "dummy" propulsor to determine the surface frictional power. This figure also shows the bare shaft power in air. It is assumed that the frictional effects of air on the bare shaft are negligible and thus that curve is taken as the power required to drive the gears in the test rig.

With those assumptions the power associated with the frictional forces on the exterior surface of the propulsor in water becomes:

Surface Frictional Power = "Dummy" Propulsor Power - Disk Power - Gear Power

Equation (3)

and plots of these results are shown in Figure 12. (The torque values can be determined from the relationship: $hp = 2\pi nT/550$ where n is the rotational speed and T is the torque.)

If one now considers the introduction of an axial flow in the direction of the axis of the rotating cylinder, the boundary layer growth should differ from the case where the cylinder is rotating at a constant rate in quiescent water. With flow in an axial direction, a "new" boundary layer is constantly being formed at the leading edge in contrast to the quiescent case where there is no "leading" edge. Consequently, for the real world case, it was postulated that the power demand would be somewhat reduced <u>provided</u> the axial flow is a reasonable percentage of the surface rotational velocity. To check this assumption, a quick test

was made just before test conclusion and, as the cover plate was not on the test section, the axial velocity was limited to a corrected axial flow of about 9.3 fps. Measurements were also made at bollard conditions and the difference between the data obtained with and without forward velocity for different rotational speeds is shown as a percentage of the bollard value in the upper plot of Figure 13. The lower plot shows the same information as a function of the inflow angle calculated from the tunnel flow velocity and the cylinder surface velocity. As can be noted, the introduction of an axial flow does have effect on surface frictional power but only at relatively large inflow angles is it appreciable. For this concept, the inflow angle would normally be less than 10 degrees, with this design it was less than 6 degrees.

Figure 14 compares the measured values of exterior surface frictional power with those calculated. The measured power values without forward velocity might be expected to be somewhat higher than those calculated because of the "no leading edge" factor mentioned earlier. Not too surprisingly, when one considers the real world factors involved, the measured values with forward velocity never exceed the values obtained without forward velocity.

Propulsor Performance

In the section on Test Equipment it was pointed out that while testing of the proposed concept considered driving powers of the order of 15 hp, there was, in actuality, a power availability of about 1/3 of that desired. Yet, in order to test the high rotational speed concept, a high rotational speed was necessary with this, in turn, requiring a high percentage of the available power just to overcome the frictional drag of the rotating shell. Consequently, because such a high percentage of the available power was necessary to overcome that frictional drag, little was available to develop thrust. In other words, it was estimated that the frictional drag of the high rotational speed shell would take of the order of 2 hp at 6000 rpm (close to the lowest rotational speed believed acceptable). With about 5 hp available, that left the order of 3 hp to overcome the internal frictional losses and produce thrust. If 15 hp had been available, the same 2 hp would have been needed to overcome the exterior frictional drag but 12 hp would have been available to overcome the internal frictional loss and produce thrust. Consequently, the performance range for which the propulsor configuration could be examined was extremely limited. Furthermore, recognizing that the "tares" would dominate the available power, there would be little chance to examine potential propulsive efficiencies. However, the purpose of the study was to gather fundamental insights re the hydrodynamic performance of the propulsor concept and it was believed that objective could be (and was) satisfied within the power restraints.

Performance of the Propulsor Alone

Figure 15 presents a comparison of the net thrust produced by various propulsor configurations as a function of propulsor rotational speed for the bollard condition. From this figure it is evident that, at least for the rotational speeds examined*, the inducer (by itself) is producing no net thrust. With the pump region consisting of the smooth interior shell, a slight positive thrust is noted and the addition of the bars (which forces the flow to acquire additional rotational velocity when compared with a smooth interior in the pump region), results in additional gains in thrust. The thrust is the highest for the Basic Propulsor (which is to be expected) since the ever increasing pitch vanes in the pump region force the water to accelerate in an axial direction in addition to acquiring rotational velocity.

The introduction of forward velocity brought about an unexpected result. As shown in Figure 16, none of the configurations produce positive thrust. It does appear as if the thrust produced by the Basic Propulsor, i.e., the configuration with vanes in the pump region has reached a minimum of thrust decrease and will show gains in thrust as the rotational speed increases. However, the power limitation prevented an examination of the propulsor performance at higher rotational speeds.

What was immediately evident and was quite disturbing is that this propulsor did not follow the thrust performance characteristics of a propeller or pumpjet. With a propeller or pumpjet, if one subjects the non-rotating unit to a flow, a drag or negative thrust develops. However, as soon as rotation is introduced, thrust is produced and, as the rotational speed is additionally increased, the "tare" drag is overcome and positive thrust results. Here however, the introduction of rotation produces an <u>increase</u> in drag — in fact, one configuration has 3 times the drag at 80 rps (4800 rpm) than that existing for no rotation!

The increase in drag associated with the introduction of propulsor rotation must result from changes in the surrounding flow field. There are (at least) two easily identifiable and probably causes. One is the development of the boundary layer on the exterior of the rotating shell while the other, and believed more important, is the radially exiting water jet. Both would present to the oncoming flow an effective increase in propulsor diameter but that resulting from the radially exiting jet would be much larger. Additional increases in the rotational speed of the propulsor would cause additional entrainment of fluid in the shell boundary layer, i.e., it would become deeper and the exiting jet would project farther into the surrounding flow field. Here again, the effect of deeper penetration of the exiting jet in the surrounding flow field

---

* The upper limit of the rotational speeds examined was determined by power limitations.

is expected to dominate. In addition to increasing the "form" drag, the lower pressure (velocity defect) region will also become larger — both in volume magnitude and pressure reduction. Now the flow from the propulsor must "fill" this velocity defect region if thrust is to result. Consequently, it is postulated that what we have here is a situation where there will be an increase in drag as the rotational speed increases until the volume of flow expelled from the propulsor is sufficient to fill the velocity and pressure defect at a faster rate than it is being created.

It is believed that the thrust data on Figure 16 substantiates this postulation. The thrust resulting from the radially exiting jet stream for configurations of the inducer only and the inducer with the smooth interior shell should be about the same — and these data points do form the same curve. The propulsor with 3 bars in the pump region should introduce the highest rotational component of the exiting jet (for the configurations tested) and, therefore, that configuration should exhibit the greatest increase in drag as the rotational speed increases — and it does. The best performance would be expected from the unit having both the inducer vanes and the increasing pitch vanes in the pump, i.e., the Basic Propulsor. For this case, the pump will be introducing an increase in axial velocity thus producing a decrease in the radial exit angle (in addition to creating an axial momentum change) and, from the figure, it can be seen that the Basic Propulsor is superior.

Performance of the Propulsor With a Shroud

It was recognized that the radial velocity components of the exiting jet had to be redirected into the axial direction if thrust was to be gained from that energy source. Consequently, the shroud shown on Figure 5 was one part of the initial test configurations. The sealing ring was added after the towing tank tests when visual observations indicated some flow was exiting forward of the leading edge of the shroud. Provisions for the installation of honeycombs to help in redirecting the rotational components of the flow were also added at that time. Two types of honeycomb were used. One was 1-inch thick aluminum hexcell made of 0.005-inch thick stock with a dimension of about 0.1-inch across the flats of the hexagon openings, the other honeycomb was of plastic with square openings 0.2-inch x 0.2-inch with a material thickness of 0.080-inch. The depth axial length was 3/4 inches. A "long tube" shroud was used in one test with the inducer only. This arrangement was shown in Figure 6. In this case, the plastic honeycomb was 1-inch long (or deep) with the same cell size openings. Identification of the honeycombs will be by the terms "aluminum" or "plastic."

Figure 17 presents a comparison of the net thrust produced by the various propulsor configurations as a function of propulsor rotational

speed in the bollard condition. This data can be compared with that of Figure 15 where the difference is the addition of the shroud. It can be noted that the addition of the shroud improved the performance of all configurations except the one having vanes in the pump portion. This was not too unexpected since, as pointed out before, the vanes in the pump portion of the propulsor increase the axial velocity and thus the radial velocity components have already been minimized to some extent.

Figure 18 presents data with the introduction of forward velocity for the same cases as shown on Figure 17. Thus, comparing Figure 17 with Figure 18 will show the effect of velocity for the shroud case while comparing Figure 16 with 18 will show the effect of shroud addition. In comparing Figure 17 with 18, what was noted in comparing Figure 15 with 16 is again evident. The introduction of propulsor rotation when a forward velocity exists does not introduce an immediate gain in thrust such as occurs with a propeller or pumpjet. However, all of the configurations indicated that higher rotational speeds would result in positive thrust, but the power limitation of the present setup prevented the establishment of that indication as an operational fact.

Static Pressure and Velocity Surveys

By placing your hand in the flow field behind the propulsor when it was operating at a bollard condition, a large "dead water" region could be felt about the axis of rotation region with high jet velocities encountered as one's hand moved away from the axis. To gain an insight as to what flow conditions did exist, a tuft was employed to gain a visual grasp of the situation. The tuft observations were then followed by a series of static pressure and velocity surveys. A sketch of the flow field as visualized from tuft observations is shown in Figure 19. As shown in the sketch, the flow exited at a relatively high angle and produced a large re-entrant jet region. Coupled with these flow movements was a rather strong rotation of the entire flow field.

All static pressure and velocity surveys were made in the horizontal plane coinciding with the axis of propulsor rotation. The surveys were started at the drive shaft axis with the pitot tube then moved in a radial (horizontal) direction. The reference static pressure was taken as that existing in the channel in that horizontal plane 6-inches away from the drive shaft axis. At this position the flow in the channel was relatively undisturbed by the action of the propulsor. When data was taken with tunnel flow velocity, the reference static pressure was obtained with the tunnel at speed but with a non-rotating propulsor. The measurements were made with a standard pitot static probe* and a water manometer. Of interest was information about the magnitude and

---

* United Sensor and Control Corporation, Model PBE-24-H-22-ON-W

extent of the lower pressure region, i.e., the base drag and the velocity defect. The static pressure fields will be examined first. While data was obtained with several configurations, emphasis was on the Basic Propulsor and that data is presented here.

Figure 20 presents two static pressure surveys for the Basic Propulsor under bollard conditions with and without the shroud. Several factors of interest are evident. The first is the significant magnitude and radial extent of the reduced pressure region when the propulsor is operating without the shroud while a second is how the shroud essentially eliminates this reduced pressure region. Note also the additional reduction in pressure (for the non-shroud case) with increasing rotational speed. It is interesting that the pressure change is ≈ proportional to ω^2, i.e., it does follow the law for a fluid in a rotating cylinder where:

$$\frac{\omega_1^2}{p_1^2} = \frac{\omega_2^2}{p_2^2} \quad \text{or} \quad \frac{\omega_1^2}{\omega_2^2} = \frac{p_1^2}{p_2^2} \quad \text{here} \quad \frac{\omega_1^2}{\omega_2^2} = .573 \quad \text{and} \quad \frac{p_1}{p_2} = .534$$

Equation (4)

Figure 21 presents the static pressure surveys for the Basic Propulsor when forward velocity is introduced. One can see the same general effect as that encountered with the bollard condition shown on Figure 20, i.e., a large reduced pressure zone for operation without the shroud and the elimination of "base drag" with shroud addition. Furthermore, the static pressure continues to change with propulsor rotational speed. Of particular interest is the increase in the magnitude of the reduced pressure (for the non-shroud case) as a result of the introduction of forward velocity. The change in the centerline pressure for the two rotational speeds is roughly the same for the bollard and forward velocity case and implies that the forward velocity superimposed an additional pressure reduction of the order 32 psf. For the shroud configuration, the pressure changes from the reference are again quite small.

Figure 22 presents the axial velocity surveys for the bollard condition taken in conjunction with the static pressure survey. These data show that for the non-shroud case the exiting annular jet of water lies well above that for the shroud case. Or to put it another way, the shroud does a reasonably good job of confining the radial expansion of the jet although a large dead water region still exists about the rotational centerline.

Figure 23 shows the velocity profiles when forward velocity is introduced for the bollard condition. It is evidence that a large wake

defect exists even at a rotational speed of 66 rps (3960 rpm). This factor, together with the reduced pressure situation shown on Figure 20 makes it understandable why no positive thrust existed as was shown on Figure 15. With the introduction of forward velocity (shown on Figure 24), the wake defect is becoming substantially filled and this fact, together with the improved static pressure situation as shown on Figure 21, explains the axial force data shown on Figure 18. In discussing the axial force data of Figure 18 it was suggested that an increase in rotational speed* would result in positive thrust and the following comments substantiate that claim. If one plots the wake defect volume (for the shroud case) as a function of propulsor rotational speed, it can be seen from Figure 25 that the wake should be filled at a rotational speed of the order of 81 rps (4860 rpm) for a corrected forward velocity of 8.5 fps. Since the geometric pitch of the helix vanes in the inducer is 1.25-inches per revolution, it follows that, from geometric considerations, the rotational speed to fill the wake should be 82.6 rps (4956 rpm), a value quite close to that resulting from the just presented calculation of the wake defect.

Transfer of Rotational Velocity to the Liquid - Background

The amount of rotational velocity transferred to the liquid passing through the propulsor is of importance because:

1. it requires energy,

2. it bears directly upon the magnitude of the low pressure in the pump region, and,

3. this rotational energy, if forming a significant portion of the total energy transferred to the liquid, must be converted into thrust assisting energy if reasonable propulsive efficiencies are to be obtained.

Hard data on the transfer of rotational velocity to a liquid passing through a propulsor of this type is lacking but, by using as a starting point, an estimate of the power required to overcome the friction acting on the exterior of the rotating propulsor, values for design considerations were established. The exterior of the propulsor is a smooth shell whereas the interior comprises a smooth inner surface plus vanes. Consequently, a power requirement of 2 x that of the exterior seems reasonable. When the propulsor is operating at a given rotational speed, the liquid passing through the propulsor must gain some angular acceleration with relationship described by:

---

* Which could not be done in the present study because of power limitations.

$$T_o = J_M \alpha \qquad \text{Equation (5)}$$

where

$$J_M = \frac{1}{2} Mr^2 \qquad \text{Equation (6)}$$

and T_o is the unbalanced torque, J_M is the moment of inertia about the axis of rotation, α is angular acceleration, M is the mass and r is the radius. Furthermore,

$$hp = \frac{2\pi nT}{550} \qquad \text{Equestion (7)}$$

where n is rotational speed and T is the torque.

Transfer of Rotational Velocity to the Liquid - Initial Assumptions

Consider an estimate made during the design stage for the model case of 100 rps. At 100 rps, the ideal flow through the propulsor should be 0.506 cfs, i.e., the pitch (0.1042 ft/rev) x 100 rev/sec x flow area (.048583 ft^2). The mass is 0.981 slugs and the radius 1.625-inches (0.1354-ft). From Figure 9 the hp for the exterior surface friction is 1.675 (1.25 kw) which is doubled in the subsequent calculations following the reasoning stated earlier. Putting these values in Equation (7) results in a torque of 2.93 lb-ft. From Equation (6), J_M = .00899 ft-lb/sec^2. Solving for α in Equation (5) results in a value of ≈326 radians (≈52 rps). Consequently, based on the assumptions made, it follows that the liquid would acquire a rotational speed of roughly 50 percent of the propulsor speed and that value seemed in line with what might be expected and was used in the design.

Transfer of Rotational Velocity to the Liquid - Test Data Comparison

The test data makes it possible to check that original assumption. Figure 22 shows the axial exit velocity profile for rotational speeds of 50 and 66 rps for two propulsor configurations in the bollard condition. Consider the propulsor with shroud and ignore the minor back flow at the centerline. Using graphical integration it is possible to determine the horsepower from the relationship

$$hp = \frac{\gamma QH}{550} \qquad \text{Equation (8)}$$

where γ is the specific weight, Q is the flow rate and H is the head ($V^2/2g$) in feet of liquid.

The calculated thrust force from the integration for 50 rps (including the minor static pressure effect shown on Figure 20) is 2.02 lbs and that for 66 rps is 3.16 lbs. From Figure 17, the measured values are 1.8 lbs and 3.0 lbs. Consequently, the thrust agreement is acceptable. The calculated thrust horsepowers are, as would be expected from the small thrust values, very low. For the 50 rps case ≈0.008 hp and for the 66 rps case ≈0.014 hp.

Figure 26 is a plot of the raw power demand of various propulsor configurations in the bollard condition. For the propulsor under consideration, the raw power is 1.28 kw for 50 rps and 2.05 kw for 66 rps. From Figure 12 it is found that the power demands for the exterior frictional effects and gearing are 0.8 kw and 1.18 kw respectively. Thus, the net power available to induce rotation of the flow becomes:

Power for Rotation = Raw Power - Thrust Power - Frictional and Gearing Power

and those values calculate to 0.472 kw and 0.856 kw respectively.

Returning to Figure 22, the calculated flow rate is 0.338 cfs for the 50 rps case and 0.394 cfs for the 66 rps case. The corresponding mass values are 0.655 slugs and 0.764 slugs. From Equation (6) the moment of inertia values are 0.006 ft-lbs/sec^2 and 0.0070 ft-lbs/sec^2. From Equation (5) the angular acceleration (α) is 185 rad/sec^2 for the 50 rps case and 217.1 rad/sec^2 for the 66 rps case. These α values correspond to ≈30 rps and ≈35 rps which compare well with the originally estimated values of 25 rps and 33 rps, i.e., the assumption that the liquid would acquire about 50 percent of propulsor rotational velocity.

Interior Pressure - Initial Assumptions

It was expected that the proposed concept would exhibit a decrease in pressure in the central part of the pump region of the propulsor. This reduced pressure region was considered an excellent "sink" for a gas exhausting turbine or as a source of "suction" for boundary layer control.

As a means of illustrating the possible value of this effect, consider a vehicle operating at a 1500-foot depth at a velocity of 100 fps. The propulsor is being driven at 333 rps (≈20,000 rpm). Assume a thrust of 1000 lbs is needed and that the overall hydrodynamic

propulsive efficiency (η) will lie between 0.60 and 0.65. Furthermore, the inside diameter of the propulsor is selected as 6-inches with an outside diameter of the driving shaft of 2-inches (inside hollow for gas exhaust). Because of its operation in the boundary layer of the vehicle, assume an average inflow velocity of 0.7 of the vehicle speed and an exit velocity of 2 x the inlet velocity to develop the thrust. The net geometric flow area, considering the shaft and propulsor vanes, is 0.16 square feet.

The force resulting from an axial change in momentum:

$$F = \eta\left[AV_{inlet}\rho(V_{exit} - V_{inlet})\right] \qquad \text{Equation (9)}$$

with the terms self-explanatory or defined earlier. Now substitute the applicable values to determine η. That will result in:

$$1000\ lb = \eta\, x(0.16\ ft^2)\ x\ (70\ ft/sec)\ x\ (2\ lb\text{-}sec^2/ft^4)\ x\ (140\ ft/sec - 70\ ft/se$$

and $\eta = 0.638$ which is within the estimate range of 0.60-0.65. Thus the basic assumptions seem valid.

An estimate of the reduced pressure was made in two ways. The first way was through the use of Equation (1) defined earlier as $y = \omega^2x^2/2g$ and redefined here as

$$\frac{\Delta p}{\gamma} = \frac{\omega^2x^2}{2g} \qquad \text{Equation (10)}$$

where $\Delta p/\gamma$ is the pressure head difference between the axis of rotation and, in this case, a point on the "free" surface of the liquid in the pump region of the propulsor, γ is the specific weight of the liquid and the other terms are as defined before. Inserting the appropriate values for the hub surface:

$$\frac{\Delta p}{64.0\ lb/ft^3} = (2094\ rad/sec)^2\ x\ (0.0833\text{-}ft)^2/64.4\ ft/sec^2$$

and the calculated pressure difference becomes ≈470 feet of sea water, if the flow is rotating at the same speed as the propulsor.

Since the flow in the pump region of the propulsor is accelerating, the water surface will move away from the axis of rotation following the relationship described by Equation (1). If, instead of the hub surface, an axial station in the propulsor is considered where the local flow has increased in axial velocity to that demanded to produce the desired thrust, the water surface will be at a radius of ≈2-inches. At that station, the difference in pressure between that existing on the axis of rotation before rotation and that after rotation is 1892-ft — again with the stipulation that the water has attained the rotational velocity of the propulsor.

It was recognized that the water would not, in fact, acquire the full rotational velocity of the propulsor but the potential improvement in open cycle gas turbine performance through a reduction in back pressure of any reasonable magnitude made the propulsor concept interesting. In presenting the line of reasoning concerning the transfer of rotational velocity to the liquid as it passed through the propulsor, it was originally estimated that the water in the pump region would acquire about 50 percent of the propulsor rotational velocity. Considering that a valid estimate, the calculated pressure head reduction in the low pressure region of the propulsor application example becomes about 475 feet of sea water. Consequently, the implications re improved open cycle turbine performance at deep depth with this propulsor are interesting.

A second method of estimating the reduction is local static pressure head was to consider the pressure acting on the hub with and without rotation, i.e., the usual hub vortex calculation made for propellers. From Reference 3 it is shown that the pressure acting at the hub surface of a propeller due to rotation is:

$$\Delta p = \frac{-\rho}{2} (2\kappa w_t)^2 \qquad \text{Equation (11)}$$

where κ is Goldstein's Kappa Function and w_t is the induced tangential velocity. Both κ and w_t are taken at the hub surface. Considering an axial station where the axial velocity is 2 x the inlet velocity, and assuming the induced tangential is 1/4 the rotational velocity* with a

---

* Believed a reasonable assumption since a heavily loaded propeller can easily have an induced tangential velocity of 0.2 of the rotational velocity at the hub. Furthermore, in this concept, not only is the inboard section heavily loaded, the purpose of the inducer portion of the propulsor is to induced rotational velocity.

k value of 1, results in a Δp value of -30,461 psf, i.e., a pressure head reduction of 476 feet of sea water. Thus, both sets of calculations result in about the same order of pressure reduction.

Interior Pressure - Test Data Comparison

One test was made of the interior pressures of the Basic Propulsor at the centerline of rotation as a function of rotational speed under both bollard and forward velocity conditions. These data are shown on Figure 27. Using the same calculation procedures as suggested in the preceding subsection, a comparison of calculated values with the measured will be made. Only centerline pressures will be examined as measurements away from the centerline were not made inside the rotating propulsor. However, evidence that the pressure does additionally decrease as one moves away from the centerline is shown in Figure 28 where data taken downstream of the exit is shown. At that plane, the flow has expanded beyond the shroud exit diameter of 3.25-inches and some mixing and back flow must exist, thus it is reasonable to assume the minimum pressure inside the propulsor would be materially less than that measured and shown on the Figure.

Consider the test model case of 90 rps. Under bollard conditions the reduced pressure is -.455 psi or -1.05 feet of water. Using the hub radius of 0.375-inches (0.0312-ft) and assuming the rotational velocity of the water has attained 50 percent of the propulsor velocity, it follows from Equation (1):

$$y = \omega^2 x^2/2g = (283 \text{ rad/sec})^2 \times (0.0312 \text{ ft})^2/64.4 \text{ ft/sec}^2$$

$$y = 1.21 \text{ ft of water (less than the reference pressure)}$$

This calculated value is in reasonably acceptable agreement with the measured data value of 1.05 feet of water. With forward velocity, the measured pressure reduction is double that for the bollard case ≈2.10 feet of water but only the bollard condition is considered in comparing the estimate with measured data since the addition of a shroud may change the influence of the exterior velocity and pressure field on the interior conditions. In other words, with a shroud, the forward velocity effect noted here as an additional reduction in pressure may change but the shroud should not affect the interior flow in the region of interest. However, if the velocity effect would hold, then the pressure reductions would be greater than those calculated.

Using Equation (11) and the same assumption, the calculated pressure reduction is:

$$\Delta p = -\rho/2\ (2\kappa w_t)^2$$

$$\Delta p = -.97\ \text{slugs/ft}^3\ (2 \times 1 \times \pi \times .75\text{-inch}/12\text{-inch/ft} \times 90\ \text{rps}/4)$$

$$\Delta p = -75.73\ \text{psf} = -1.21\ \text{ft of water}$$

which agrees with the calculation of Equation (1).

Shroud Effectiveness

During the design stage it was recognized that a good share of the total power would go into introducing rotation to the liquid as it passed through the propulsor. That rotational energy would, of course, cause the water sheet exiting from propulsor to expand in a radial direction. To recover that energy, that radially expanding water sheet had to be redirected. A shroud was therefore designed which would redirect the radial velocity components into axial ones. That shroud was shown in Figure 5. However, the basic shroud would have but a frictional effect on the rotational velocity component. Consequently, provision was made for the insertion of honeycomb elements. The principal purpose of the honeycomb was to redirect the rotational velocity components and, in doing so, raise the local static pressure. The shroud did have an effect on the static pressure field for both the bollard and forward velocity conditions and those effects were pointed out in discussing the data on Figures 20 and 21. If the static pressure distribution shown on these figures for the 66 rps case are graphically integrated over the shroud area there is a gain in thrust of ≈1.8 lbs for the bollard condition and ≈2.8 lbs for the case with a forward velocity of 9.0 fps. Thus the shroud is converting some of the non-axial velocity components into increased local static head. What is of particular interest is that the effectiveness apparently increases with forward velocity.

Venting to the Low Pressure Region in the Propulsor

The low pressure region in the pump portion of propulsor would create a drag and in an actual application was to act as a "sink" for turbine exhaust. For these tests a hole was bored in the center of the drive shaft to a point inside the lower unit where radial holes connected this center hole passageway to a line exiting below the drive motors. A selonoid valve was attached to this line so that the line was either open or closed. It was hoped that by opening the valve, atmospheric air would vent into the low pressure region.

Now the rotation of the hollow drive shaft together with its radial holes acts like a centrifugal pump. Consequently, when the valve was opened, water was pumped out of the line (under certain conditions) because the rotational speed of the propulsor never was high enough to create a pressure low enough at the end of the drive shaft to overcome this pumping action.

When taking velocity and static pressure surveys with a forward velocity, air would vent into the propulsor from the surface of the water via the cavity formed by the pitot tube. Under these conditions, i.e., when air from the surface entered the low pressure region, the thrust would increase by the order of 5 to 10 percent. Consequently, the concept of venting into the low pressure region with a resulting gain in thrust seems justified provided the appropriate operating conditions are established.

Cavitation

The propulsor was viewed under various operating conditions and only the slightest bit of cavitation was observed at the outer leading edges of the inducer vanes. This slight cavitation could not have affected performance in any way. Furthermore, rather than machining an airfoil shaped leading edge, the edges were merely hand filed to a smooth contour. Thus this slight cavitation could be eliminated by introducing a better shape. The premise that cavitation free performance is possible is therefore believed valid.

PROPULSOR DESIGN

In the design of the test propulsor a number of assumptions were made regarding the prediction of shell surface frictional effects, the rotational acceleration of the water as it passed through the propulsor and the magnitude of the reduced pressure zone. From the data and discussion presented in this report it can be seen that the original assumptions were well founded and can be used in the prediction of those hydrodynamic performance characteristics. The thrust performance was not good and that fact was surprising since it was based upon the well established change in momentum principle. It was evident that something unexpected was happening when the thrust performance at a fixed forward velocity was examined as a function of increasing rotational speed. As pointed out earlier in this report, if a non-rotating propeller or pumpjet is subjected to a forward velocity, thrust is produced as soon as rotation begins. With this

propulsor, the introduction of rotational velocity increases the drag. This occurs for configurations with and without a shroud (see Figures 16 and 18).

It has been pointed out that the growth of the boundary layer on the exterior of the rotating shell and the radial velocity components in the exiting jet would create an effective increase in form drag which may be responsible for the observed increases in drag. With a (honeycomb) shroud, the Basic Propulsor shows but a slight increase in drag as the propulsor rotates — more than likely because the exiting jet from the shroud is being fairly well directed in an axial direction. However, the high rotational speed which is necessary before the tare drag of the unit is overcome is believed a result of the wake created by the propulsor itself. Figure 29 shows the velocity and static pressure wake surveys for the test rig (at two axial locations) and for one representative configuration of the propulsor. It follows that the propulsor must essentially* fill its own wake before it can produce thrust and the senior author neglected to consider the wake of the propulsor itself in estimating the necessary flow rate and velocity change to produce the desired thrust.

Figure 30 compares various calculated and measured flow rates for the Basic Propulsor as a function of rotational speed at a normalized forward velocity of 9 fps. What is shown here is that for this velocity, about 76 rps would be required to fill the wake and produce a neutral "tare drag" condition. Referring to Figure 18, it is seen that (for this configuration) the tare thrust condition has also been reached. Consequently, it seems necessary to include, as a part of the design process, an estimate of the wake defect created by the propulsor in establishing the necessary flow rate and velocity change in the propulsor to produce thrust.

Because this configuration operates so far "off design" as a result of not considering the wake of the propulsor in formulating the design, an examination of the conventional K_T, K_Q and η relationships must be viewed with caution. However, those parameters are shown in Figure 31 for the Basic Propulsor with the plastic honeycomb shroud.

---

* The term "essentially" is employed because thrust can be produced w/o "filling the wake" depending upon the velocity distribution.

SUMMARY

The concept of the ultra-high rotational speed propulsor examined in this study appeared to offer a number of advantages for certain underwater vehicle applications. The expected operational characteristics of the propulsor entered into areas where little hard data was available. Consequently, the thrust of the study was directed at obtaining experimental evidence which could be used in the establishment of guidelines for the future development of the concept.

There were four major areas of concern: the frictional power demand of the exterior surface of the high rotational speed shell, the transfer of rotational velocity to the liquid as it passed through the propulsor, the magnitude of the low pressure region and the development of thrust. Because of the need of a high rotational speed to investigate the first three areas of concern and the fact that there was a limited power supply, the thrust aspect (from the standpoint of potential operational efficiencies), could not be effectively examined in this study. However, the development of thrust is based upon momentum change considerations, a relationship which is well understood and, therefore, the lack of that specific information is not considered a serious shortcoming although hard data on potential propulsive efficiencies are needed. Believed more important, at least at this stage of conceptual development, is that the hypothesis describing the general hydrodynamic performance of this propulsor has been verified.

The power demand of the frictional effect on the exterior of the rotating shell is slightly higher than that predicted by the flat plate drag relationship where the shell diameter is taken as the length term and the rotational velocity is taken as the velocity term. The frictional drag predicted by employing the flow path of a fluid element based upon the vector relationship of the axial and rotational velocities is far too high. The axial velocity has an appreciable effect only when the geometric flow angle, i.e., arc tan: axial velocity/rotational velocity, is larger than about 10 degrees. From operational considerations, the angle will be less than that.

The transfer of rotational velocity is such that (for the Basic Propulsor configuration) the liquid acquires roughly 50 percent of the propulsor rotational speed. The power demand is roughly 2 x that required by the frictional effects of the shell exterior surface and is in line with wetted surface area. (The interior has the interior shell surface plus vanes.)

The magnitude of the low pressure region in the aft portion of the propulsor is related to two factors. The first is the rotational velocity of the liquid. Using that velocity, either the relationship employed in propeller design to predict the hub vortex pressure or that predicting the pressure head change on the free surface of a

liquid in a rotating vessel results in reasonably good agreement between theory and experiment. The second factor is that the reduction in pressure becomes larger with increases in forward velocity but the velocity range which could be examined in this study was too small to establish a particular relationship.

A major difference exists in the design considerations for the development of thrust by this propulsor when compared to propeller or pumpjets. With propellers or pumpjets, if a non-rotating unit is subjected to a reasonable forward velocity, thrust is developed as soon as power is supplied and rotation begins. With this concept, thrust was not produced until relatively high rotational speeds were attained.

The primary cause for this operational anomaly was the failure to consider (in the design process) the large wake (or velocity defect region) created in the flow field by the presence of the propulsor (itself). This velocity defect region must be filled* before thrust can be produced. Consequently, during the design phase of this propulsor concept the flow required to "fill" the wake of the propulsor must be included when the flow rate and momentum change necessary to produce the desired thrust is established. The failure to include that consideration, coupled with the power limitation, is the reason for the thrust performance exhibited by the configuration tested.

The increase in drag which occurred as propulsor rotation began is believed a result of the development of the boundary layer on the exterior surface of the rotating shell and the radial components of the exiting jet. Both phenomena should increase the effective form drag of the propulsor. While the drag increase was relatively small for the best of the configurations tested, this aspect must be included as a design factor.

ACKNOWLEDGMENT

The authors wish to thank Dr. Thomas E. Peirce (NAVSEA 63R Technical Monitor) and Dr. Bruce Johnson (Head, Hydromechanics Laboratory, USNA) for their interest, advice and stimulating comments offered during the test program and review of the data. Particular thanks must be given to the staff of the Hydromechanics Laboratory, so many of which contributed their specific "as needed" talents during the tests. Special recognition is made of the contributions of Mr. Donald Bunker who was the principal assistant.

---

* See Page 23 for additional discussion.

PROPOSED FUTURE EFFORT

Of the four major power demand areas of concern associated with this propulsor concept, relationships have been tentatively established for three of them and a shortcoming in the procedure employed in the estimation of thrust production identified. The accepted power limitations of this test arrangement placed recognized restraints upon the rotational speed range which could be investigated. The next phase should include a revised propulsor design incorporating the knowledge gained and the use of a power source permitting an increase in the rotational speed by a factor of 4 to 5. This higher rotational speed capability will permit an investigation of the aforementioned relationships into ranges compatible with practical application.

TECHNOLOGICAL FORECAST

The performance of the test propulsor agreed well with the conceptual postulation. The postulation envisions rotational speeds of 20,000 - 30,000 rpm (thereby permitting direct coupling to a turbine), cavitation free performance and, for a typical application, an internal flow pressure reduction region equivalent to the order of 500-ft of sea water. This pressure reduction could serve as a means of reducing the back pressure of an open cycle gas exhaust turbine or as a means of introducing afterbody boundary layer control. These data establish performance relationships which fulfill the postulation. However, testing could only be performed to rotational speeds of the order of 6000 rpm. Consequently, verification of the established relationships is necessary at higher rotational speeds to insure applicability under real world situations.

REFERENCES

1. "International Towing Tank Conference Catalogue of Facilities Published by the Information Committee of the 16th ITTC."

2. Granville, Paul S.: "Drag and Turbulent Boundary Layer of Flat Plates at Low Reynolds Numbers," Naval Ship Research and Development Center, Report 4682, December, 1975.

3. McCormick, B. W.; Eisenhuth, J. J.; Lynn, J. E.: "A Study of Torpedo Propellers - Part I," Pennsylvania State University, Report No. NOrd 16597-5, March 30, 1956.

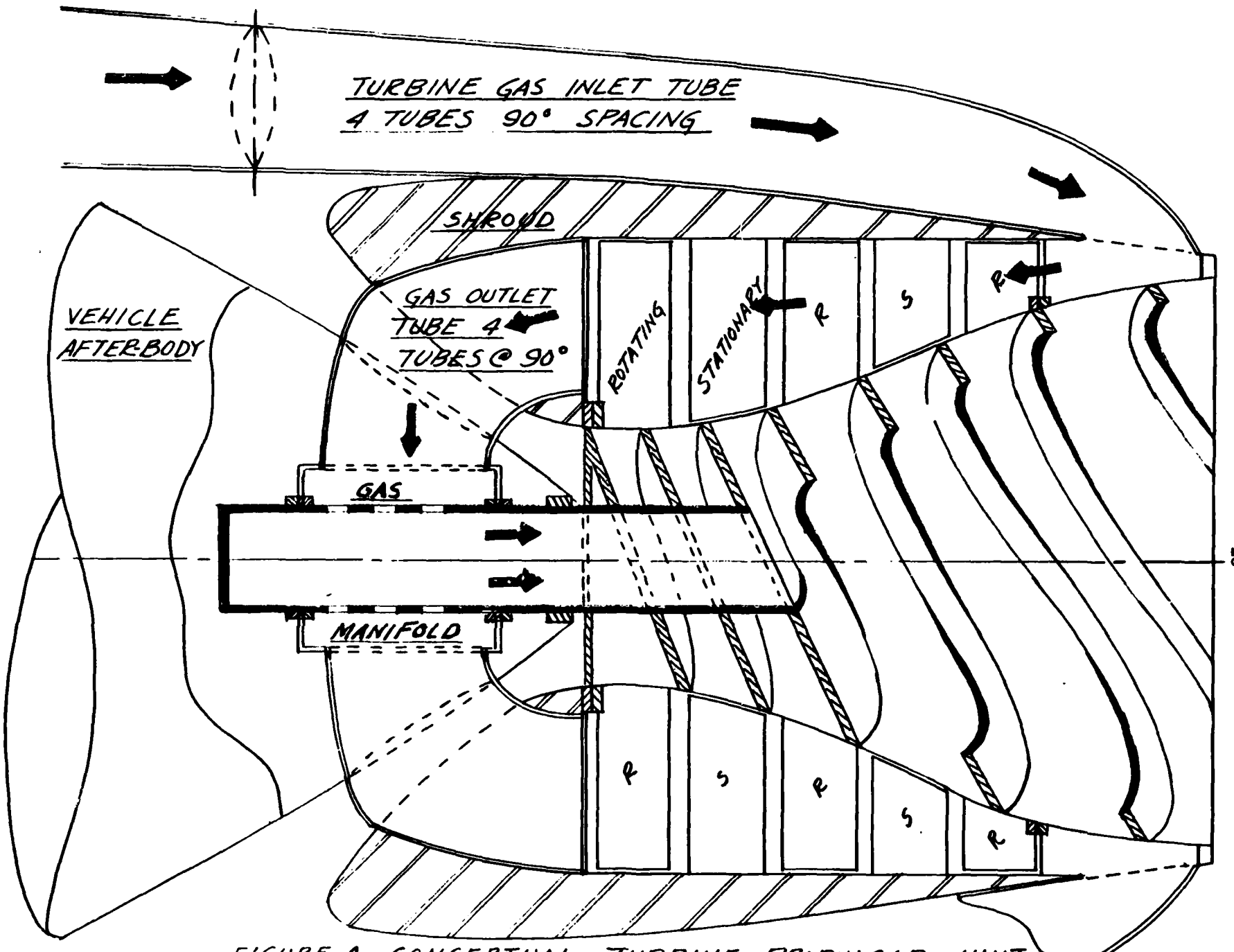

FIGURE 1 CONCEPTUAL TURBINE-PROPULSOR UNIT
ILLUSTRATING REVERSE FLOW GAS PATH

Dwn 8.2.78

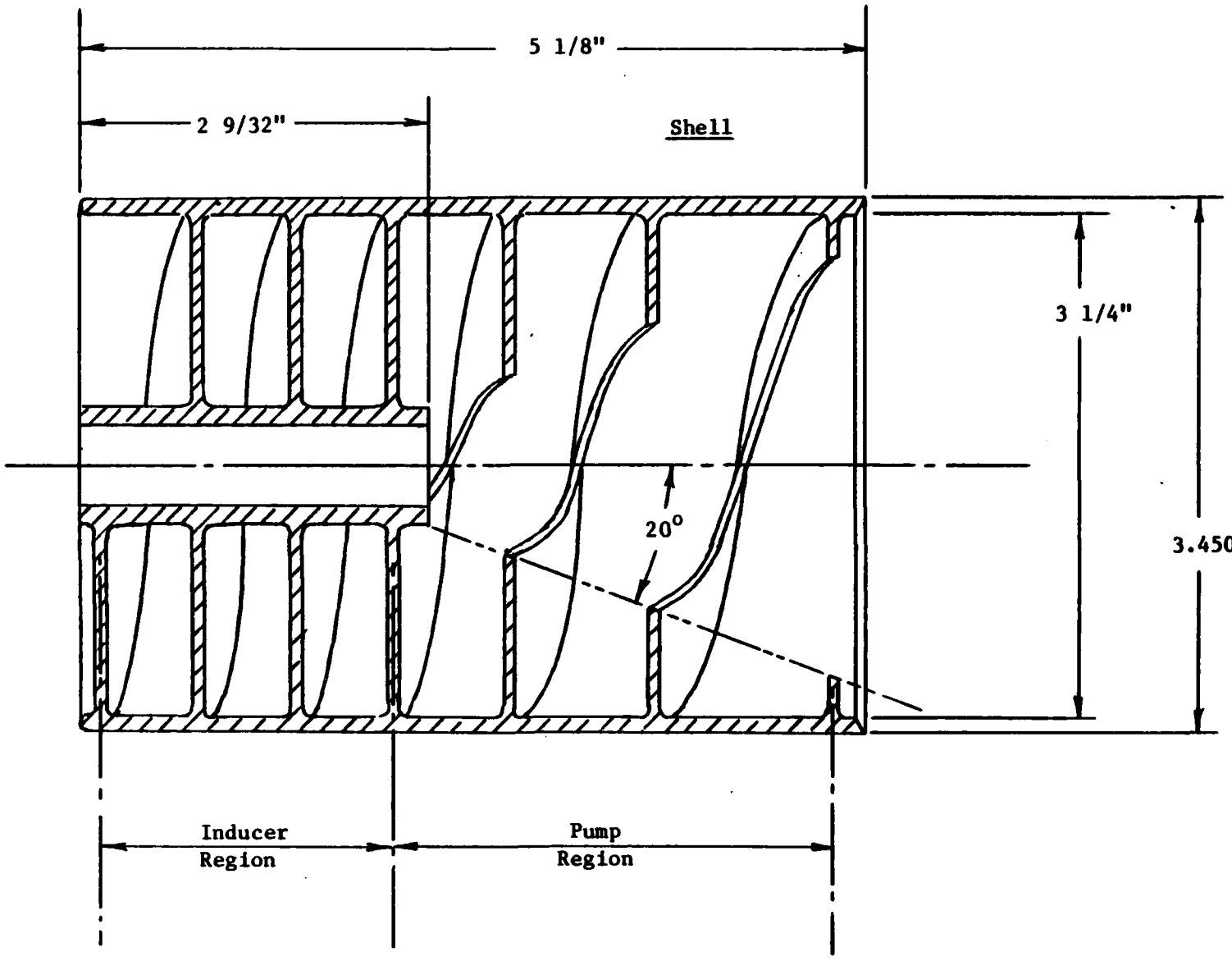

Figure 2 Cross Section of Basic Propulsor

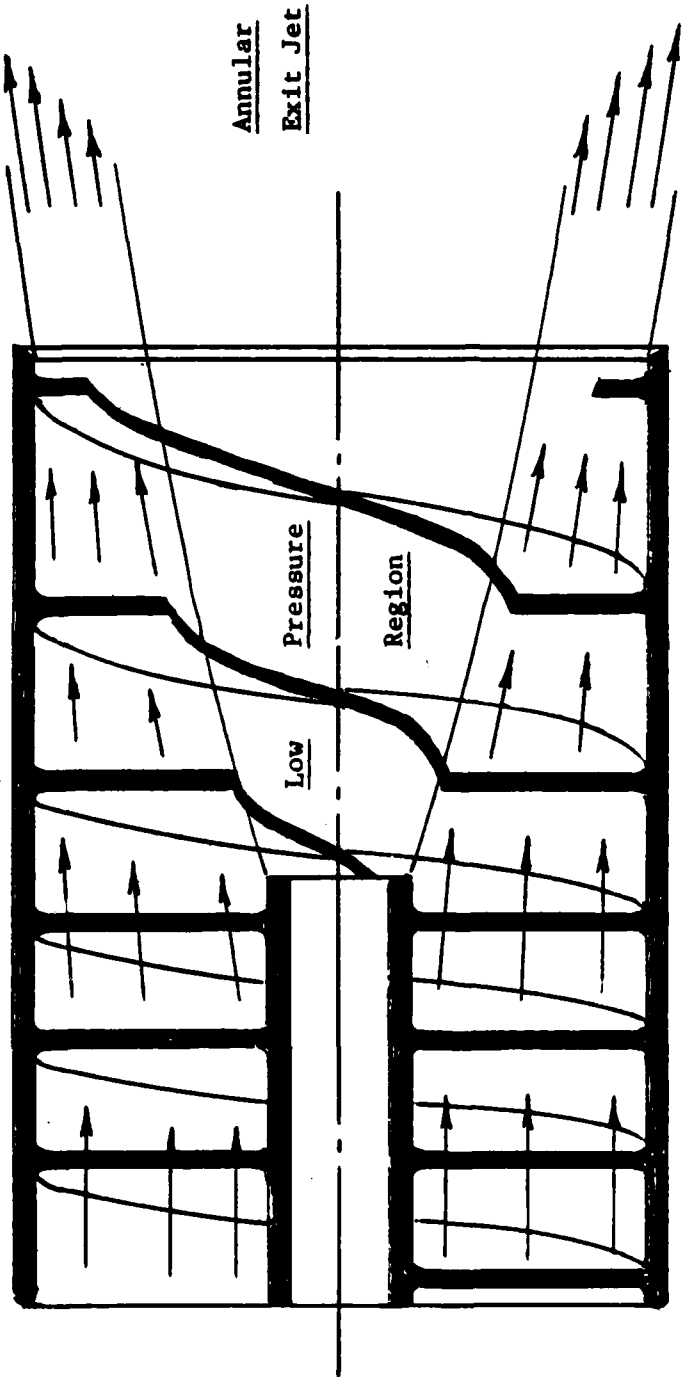

Figure 3 Sketch of Axial Water Flow Path

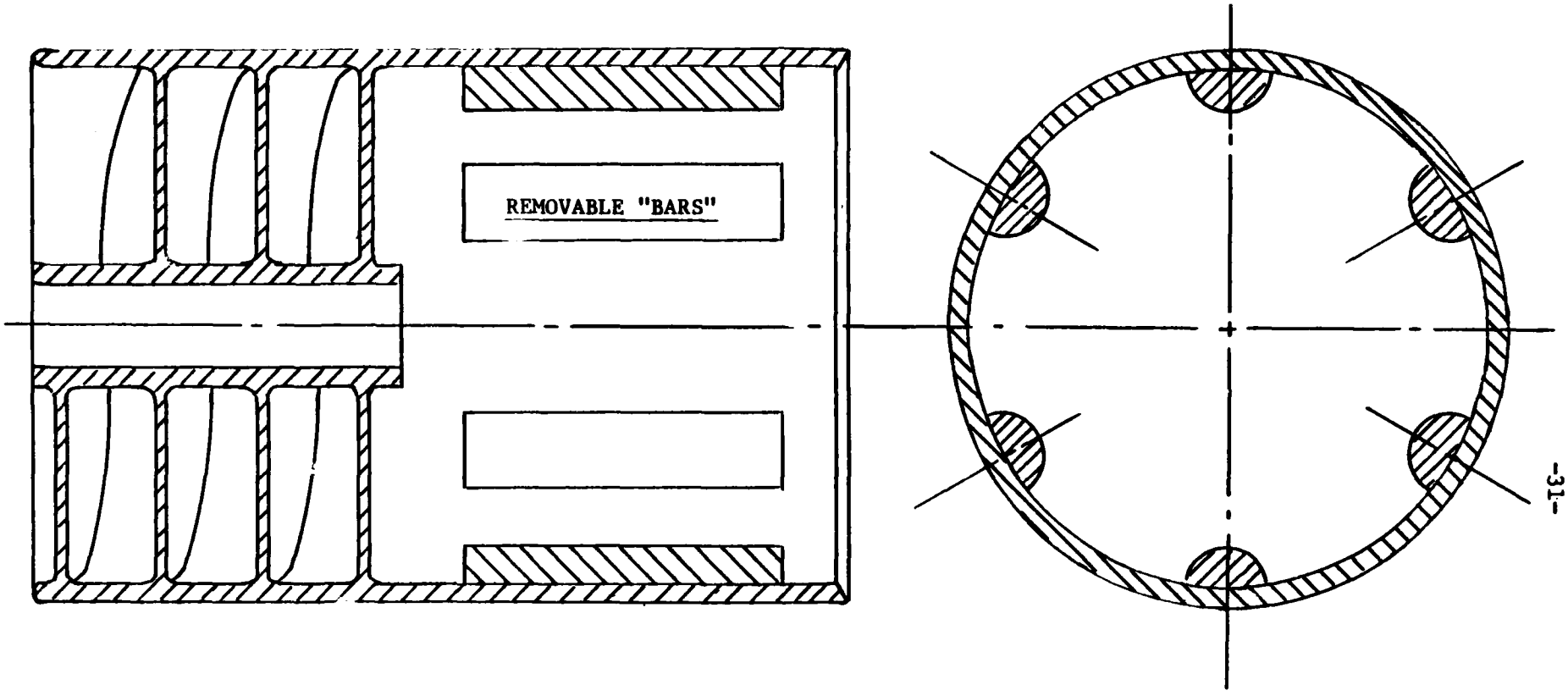

Figure 4 Sketch of Propulsor Allowing Modifications in Pump Region

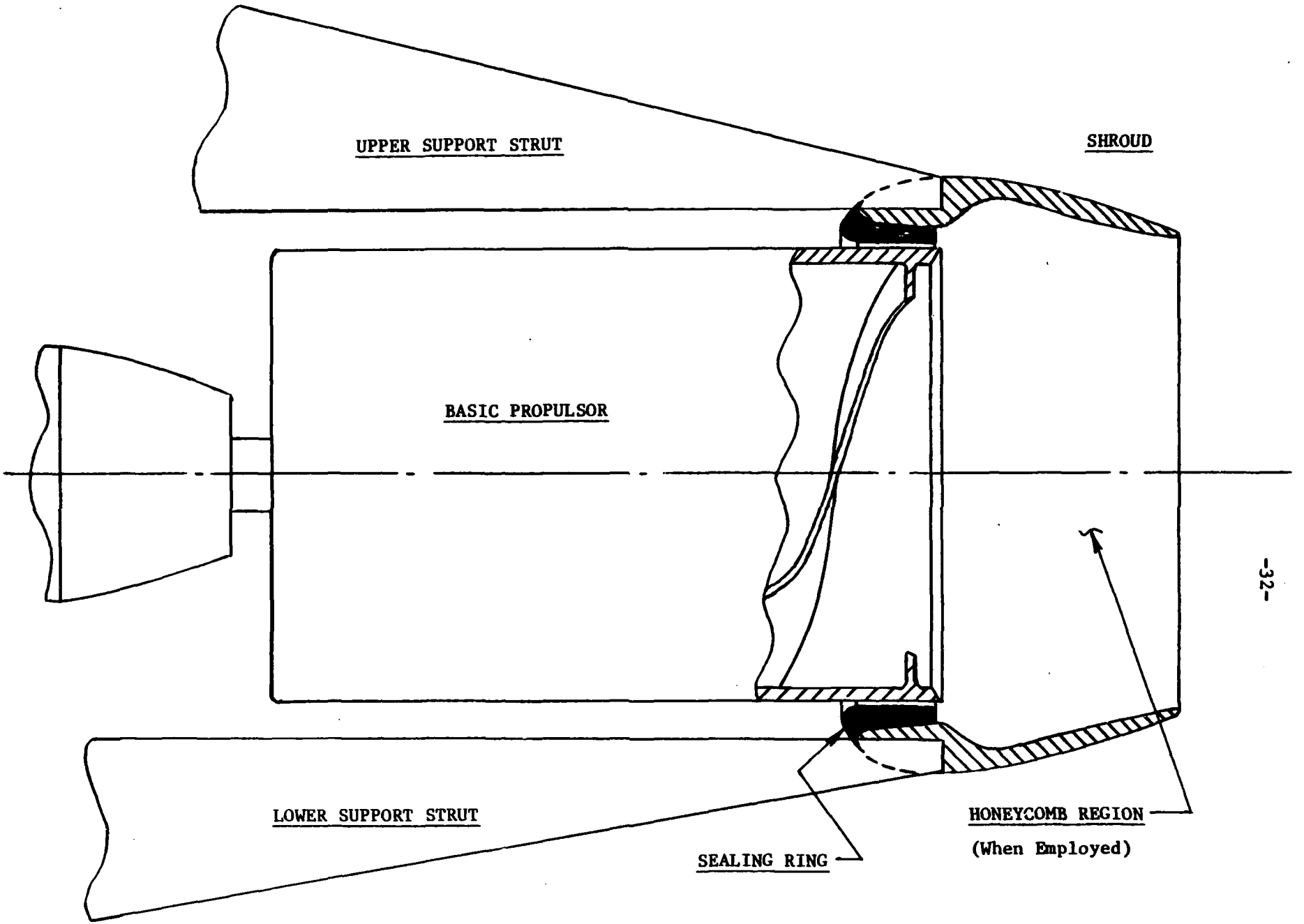

Figure 5 Sketch of Basic Propulsor With Shroud

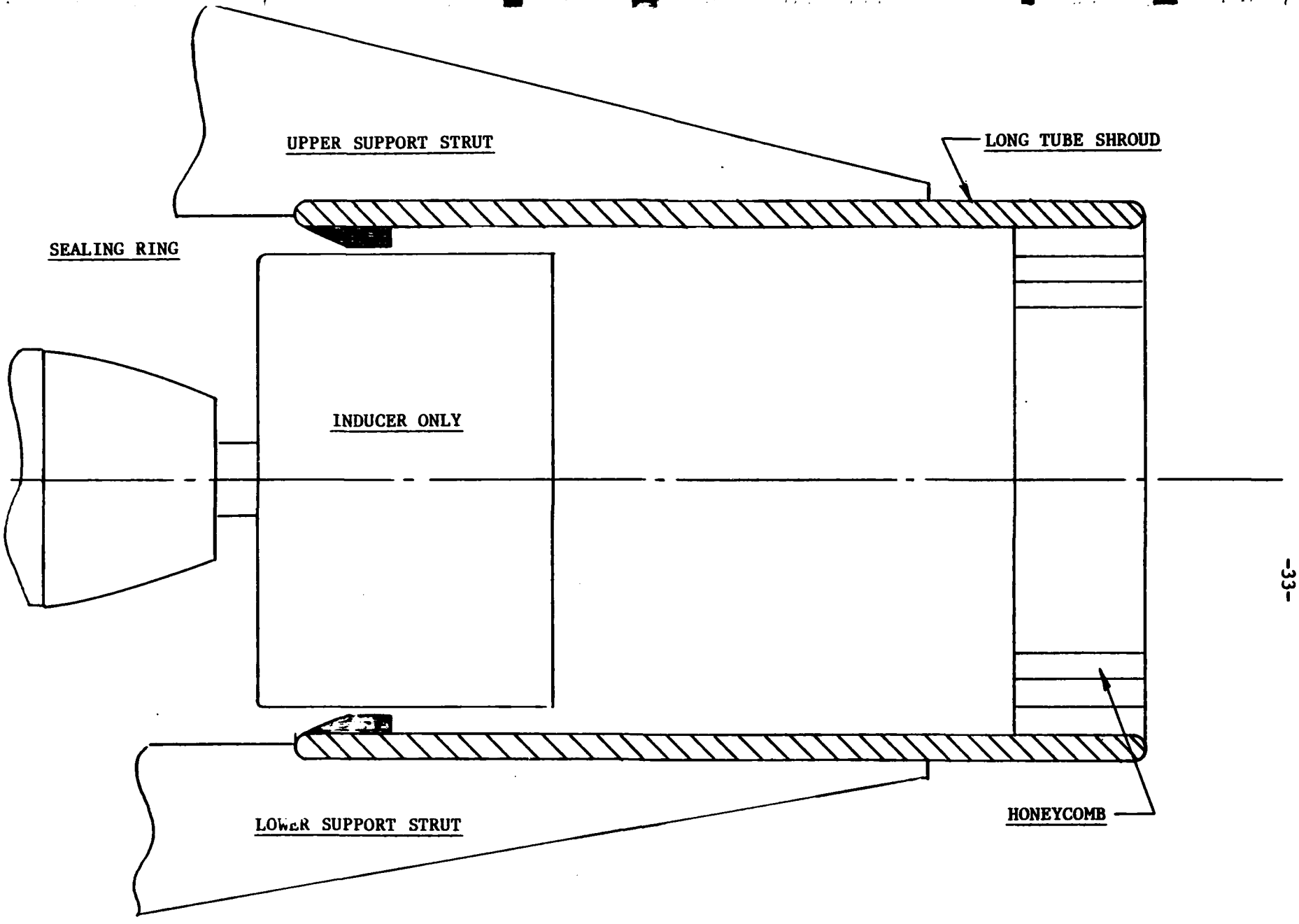

Figure 6 Sketch of Inducer Only with "Long Tube" Shroud

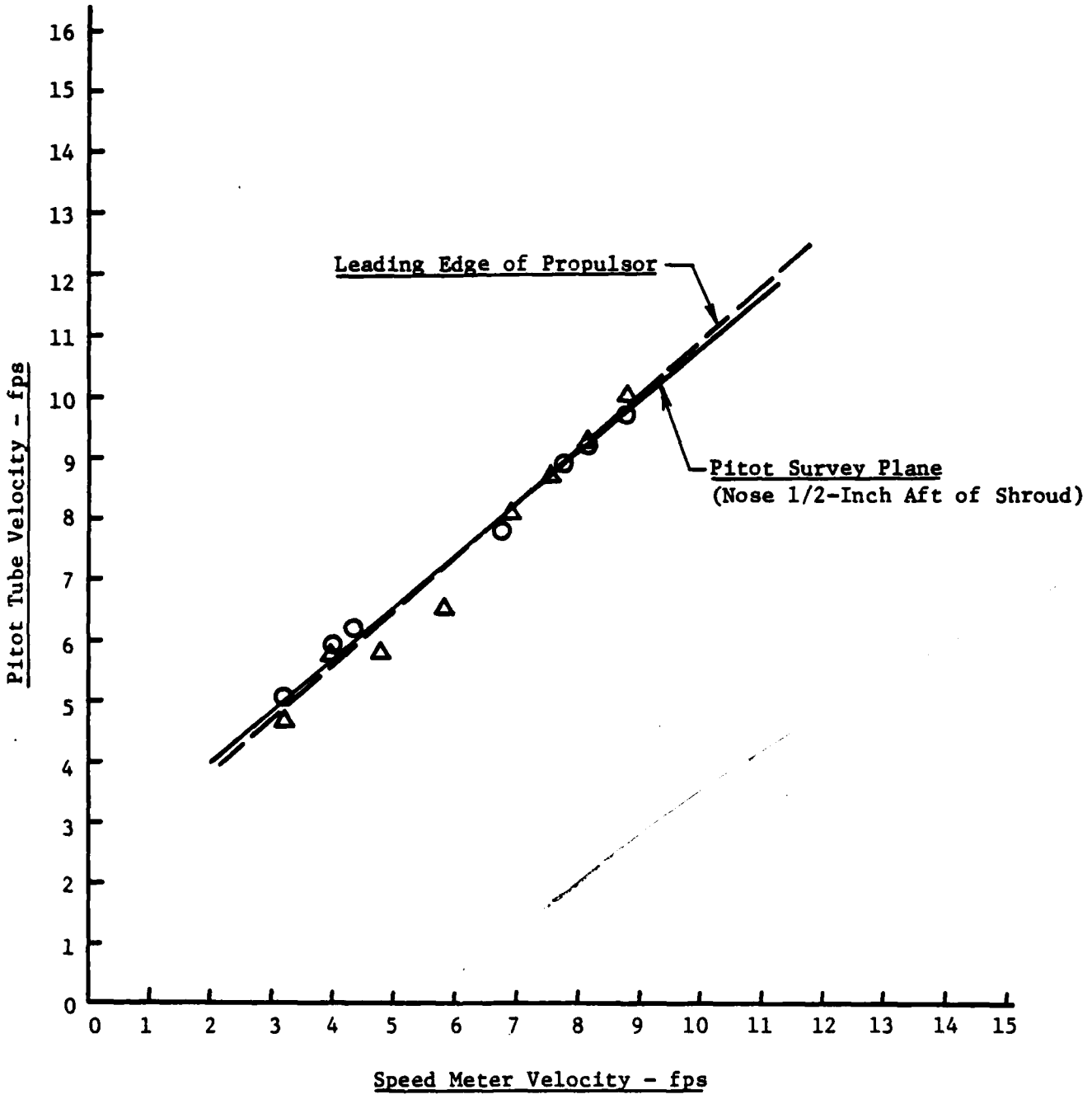

Figure 7 Comparison: Speed Meter vs Pitot Tube Velocities with Basic Propulsor and Shroud
No Propulsor Rotation

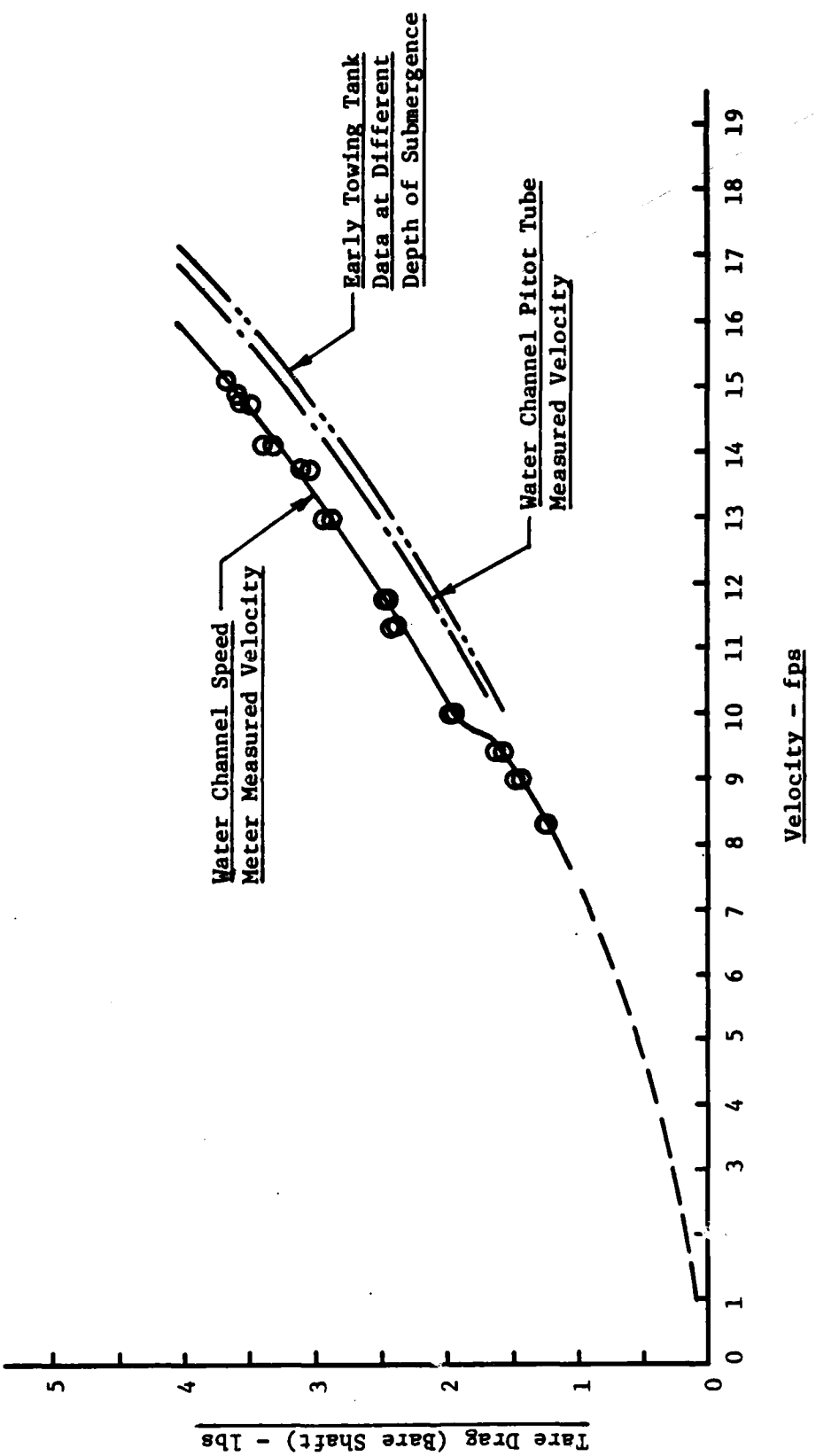

Figure 8 Basic Unit Drag vs Velocity

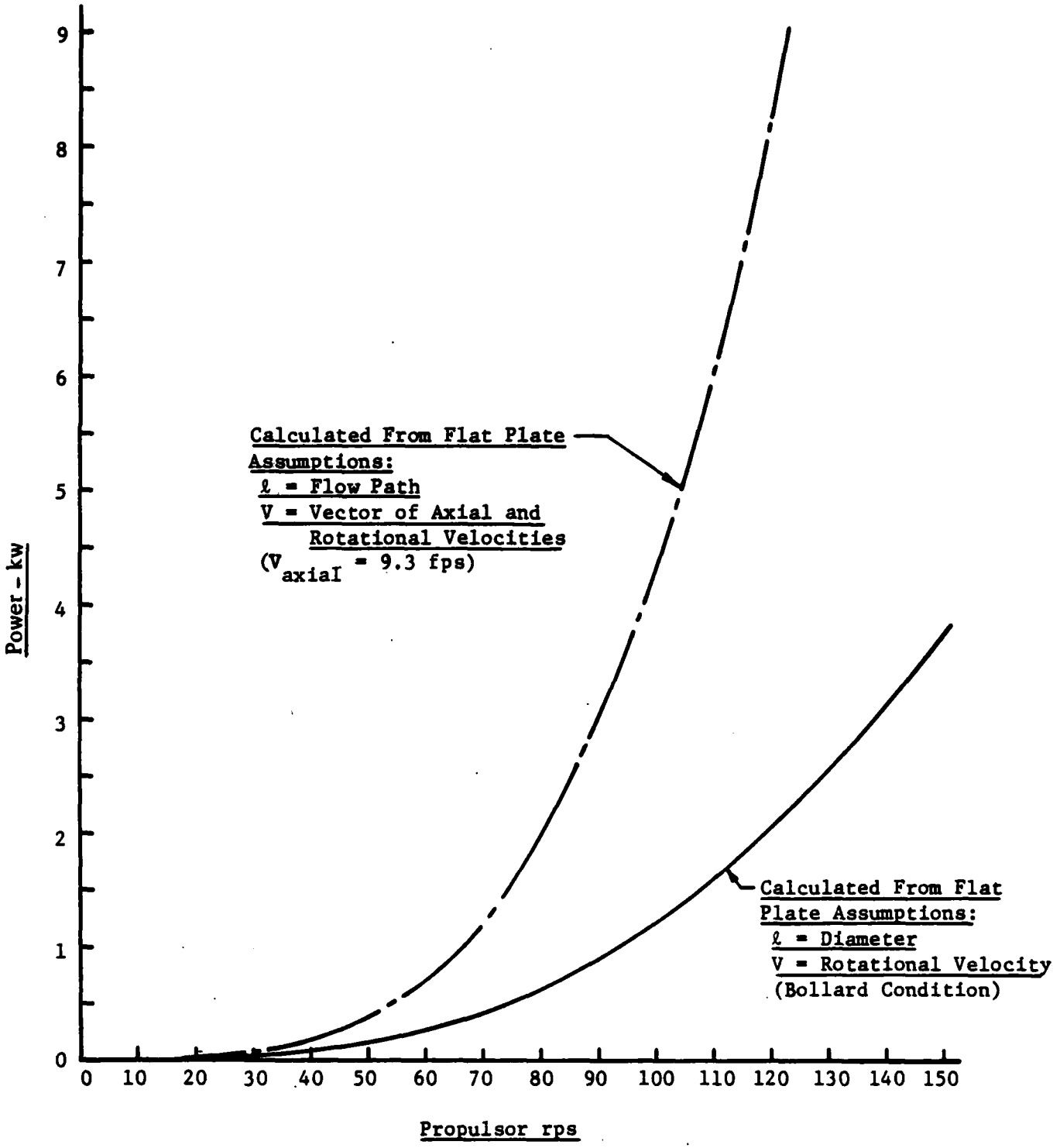

Figure 9 Predicted Power Demand for Frictional Resistance: Exterior Surface of Basic Propulsor

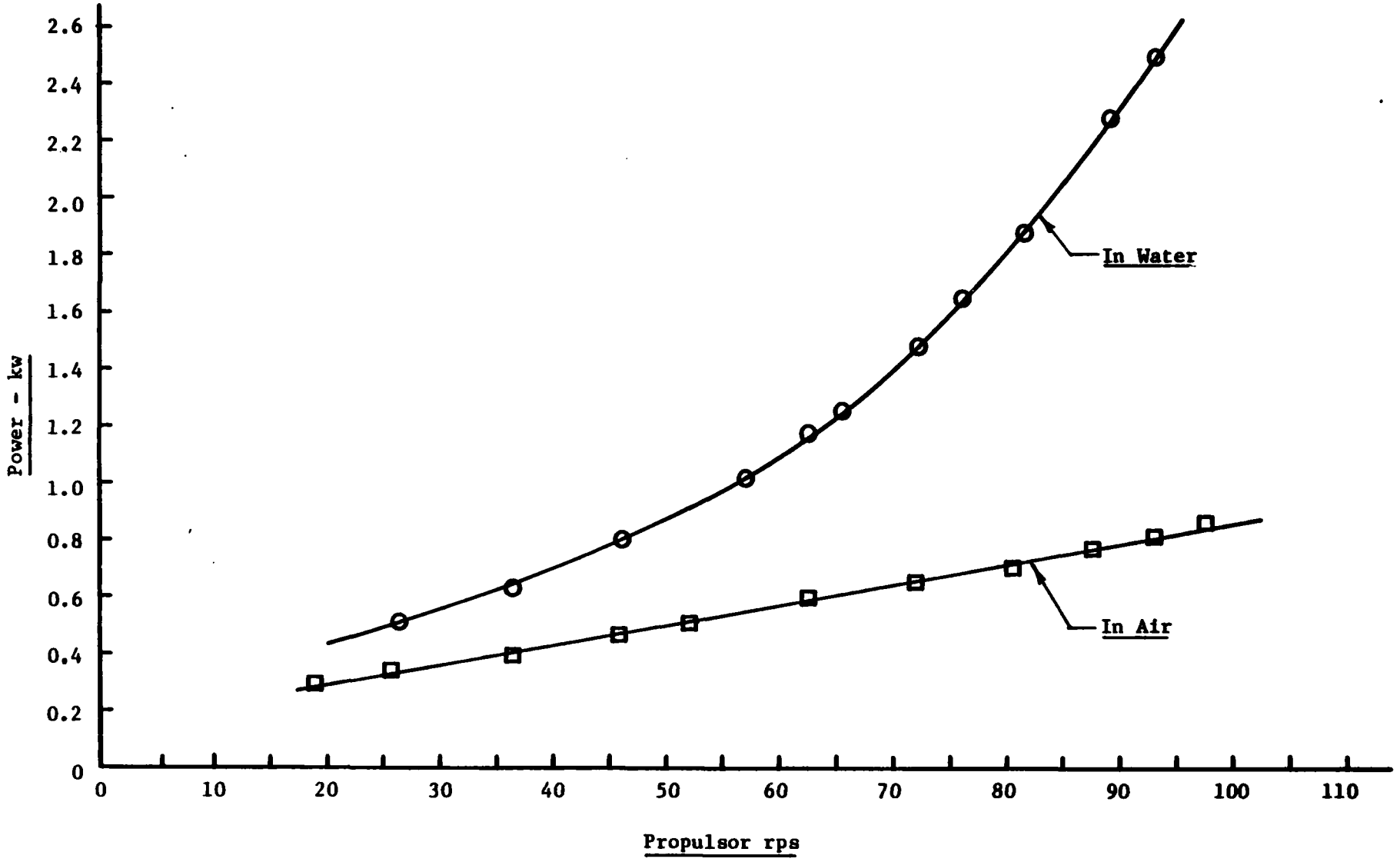

Figure 10 Dummy Propulsor Power Demand. No Shroud - Bollard Condition

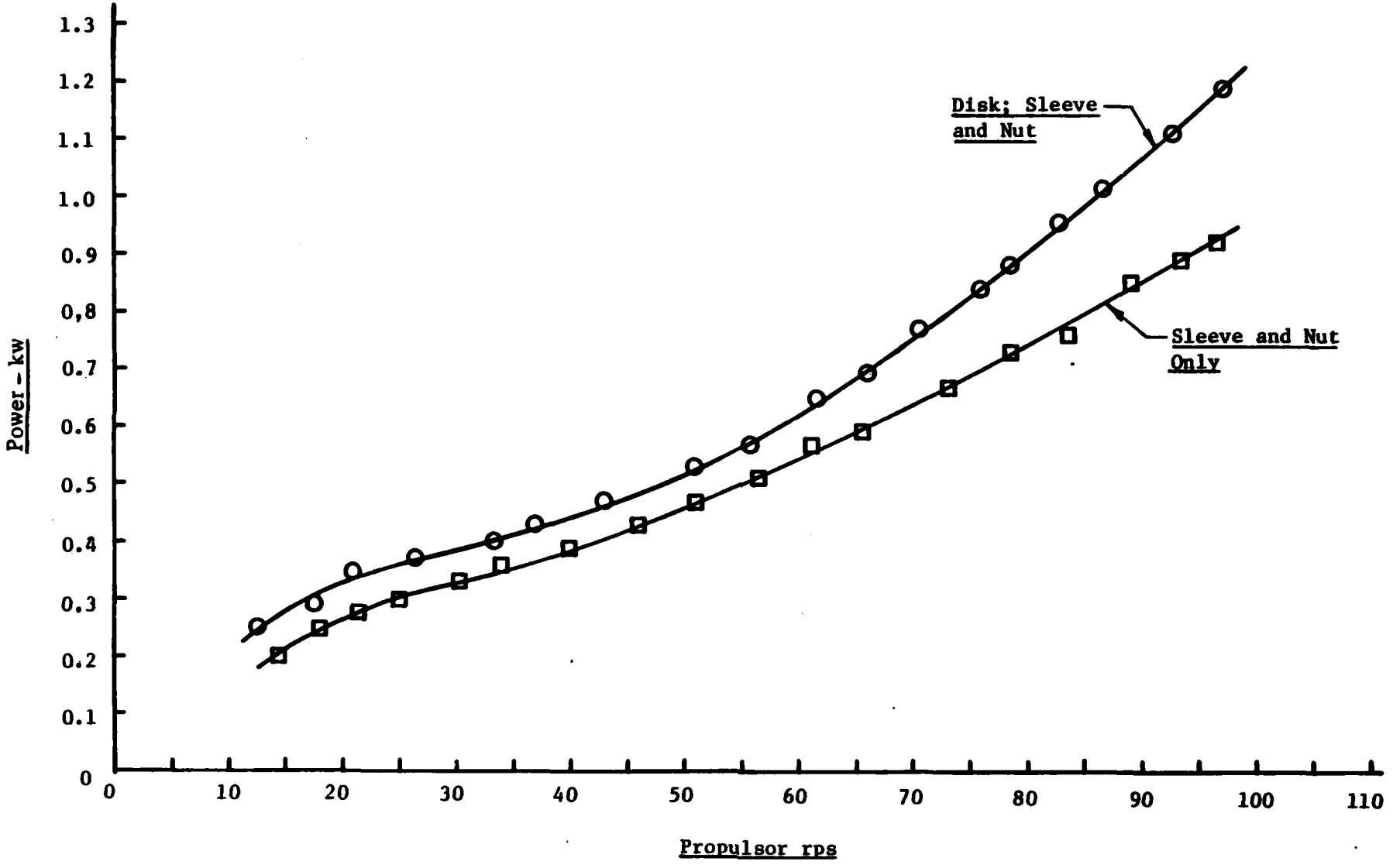

Figure 11 Surface Friction Power Demand - Thin Disk. Thin Disk Dia. = Propulsor Dia.

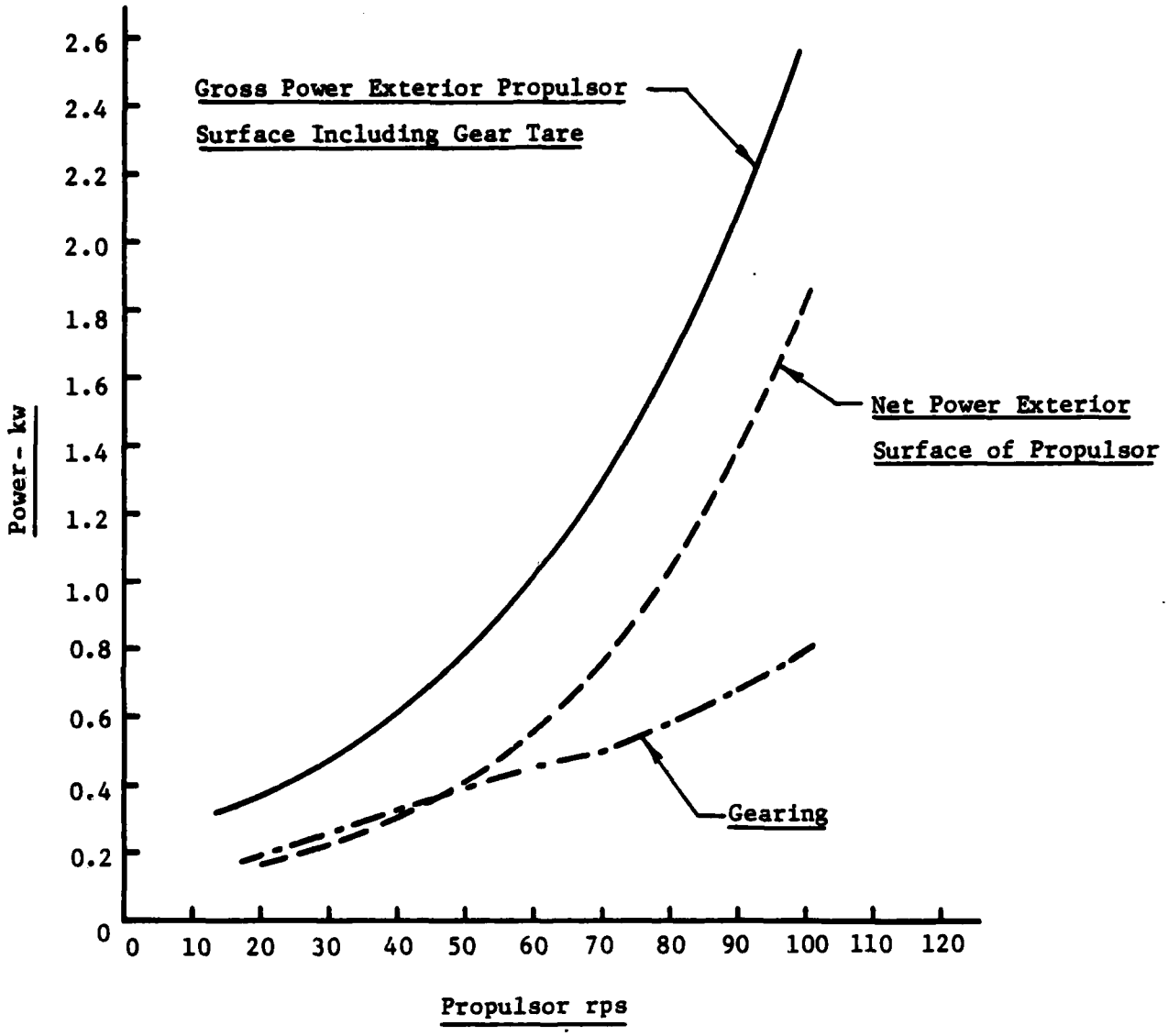

Figure 12 Propulsor Suface, Friction and Gearing Power Demands - Bollard Condition

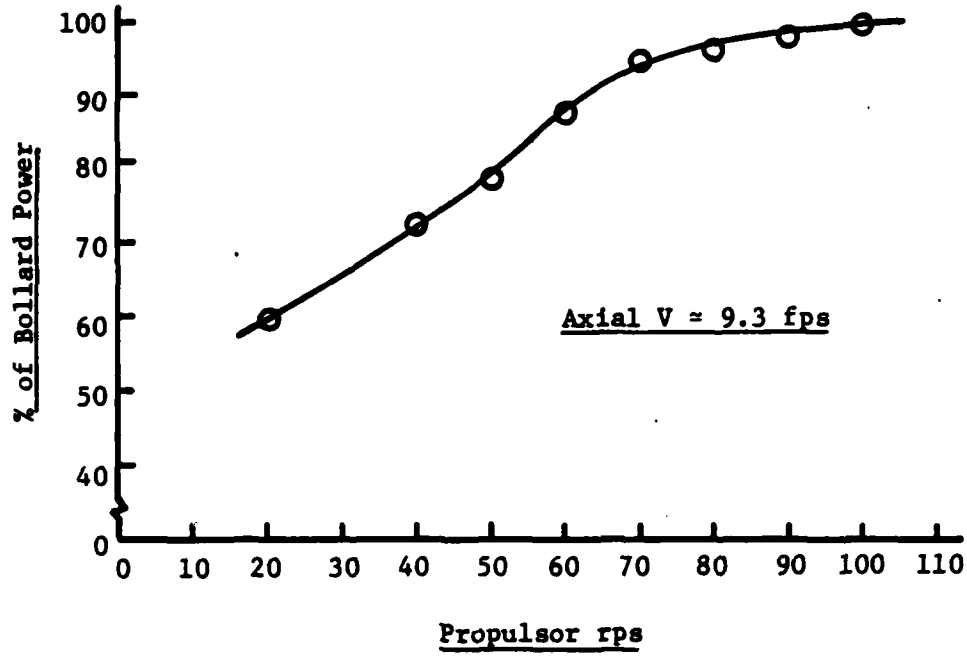

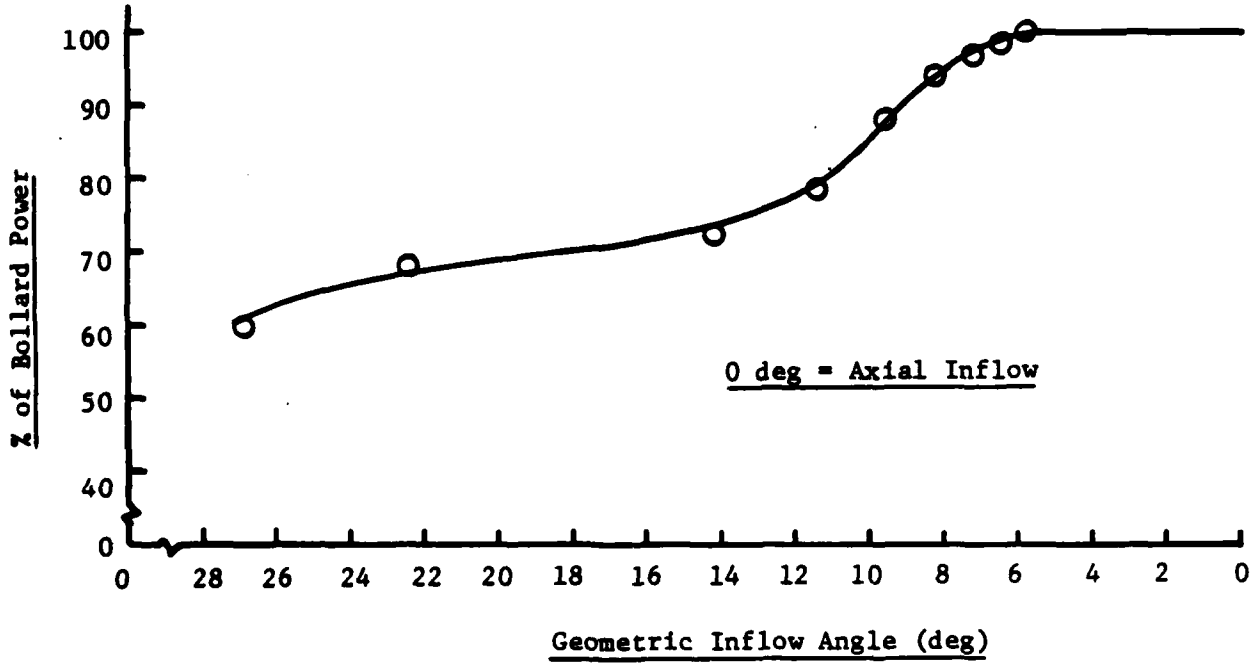

Figure 13 Effect of Axial Flow on Rotating Shell Frictional Power Demand

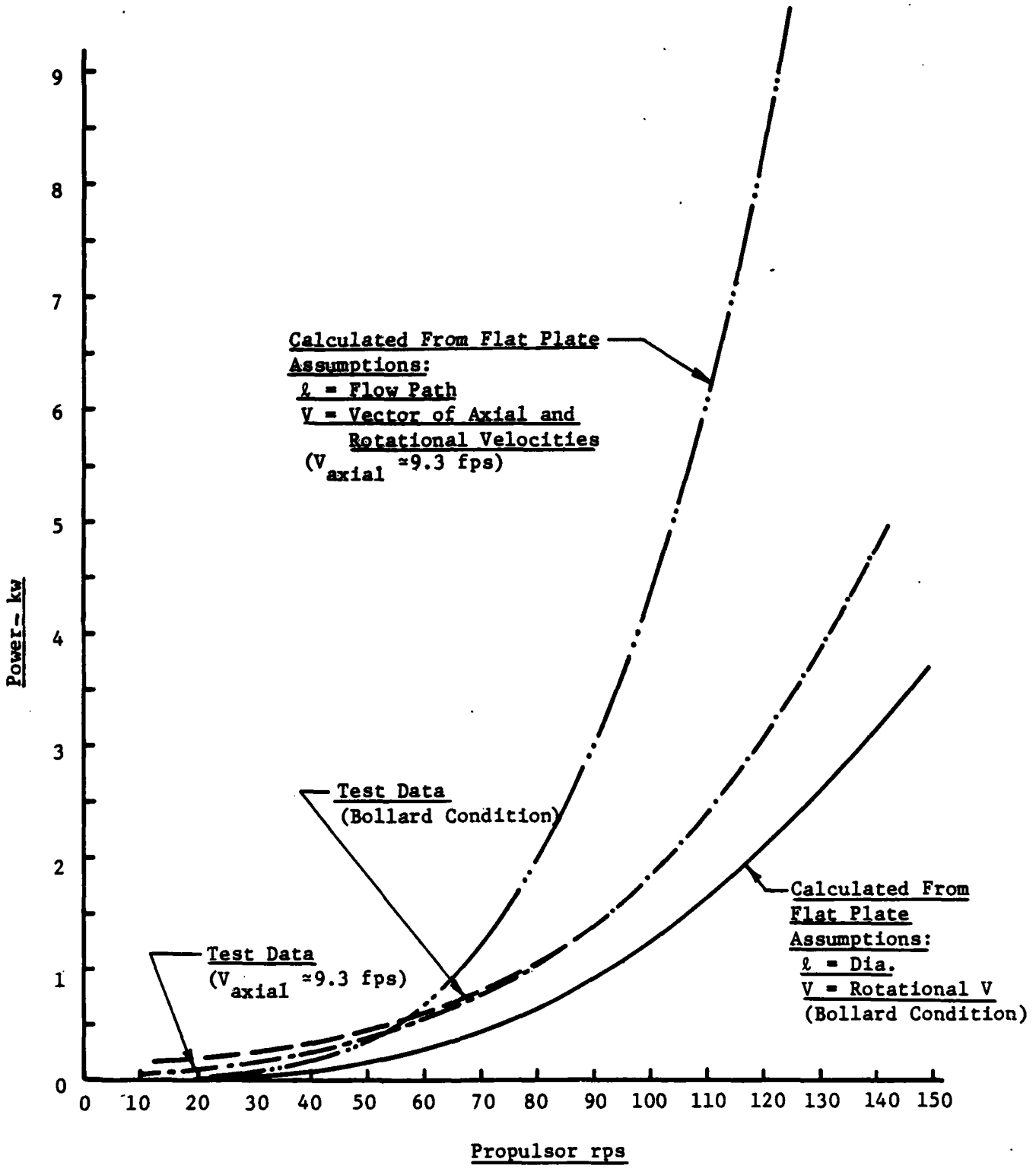

Figure 14 Power Demand of Frictional Resistance: Exterior Surface of Basic Propulsor

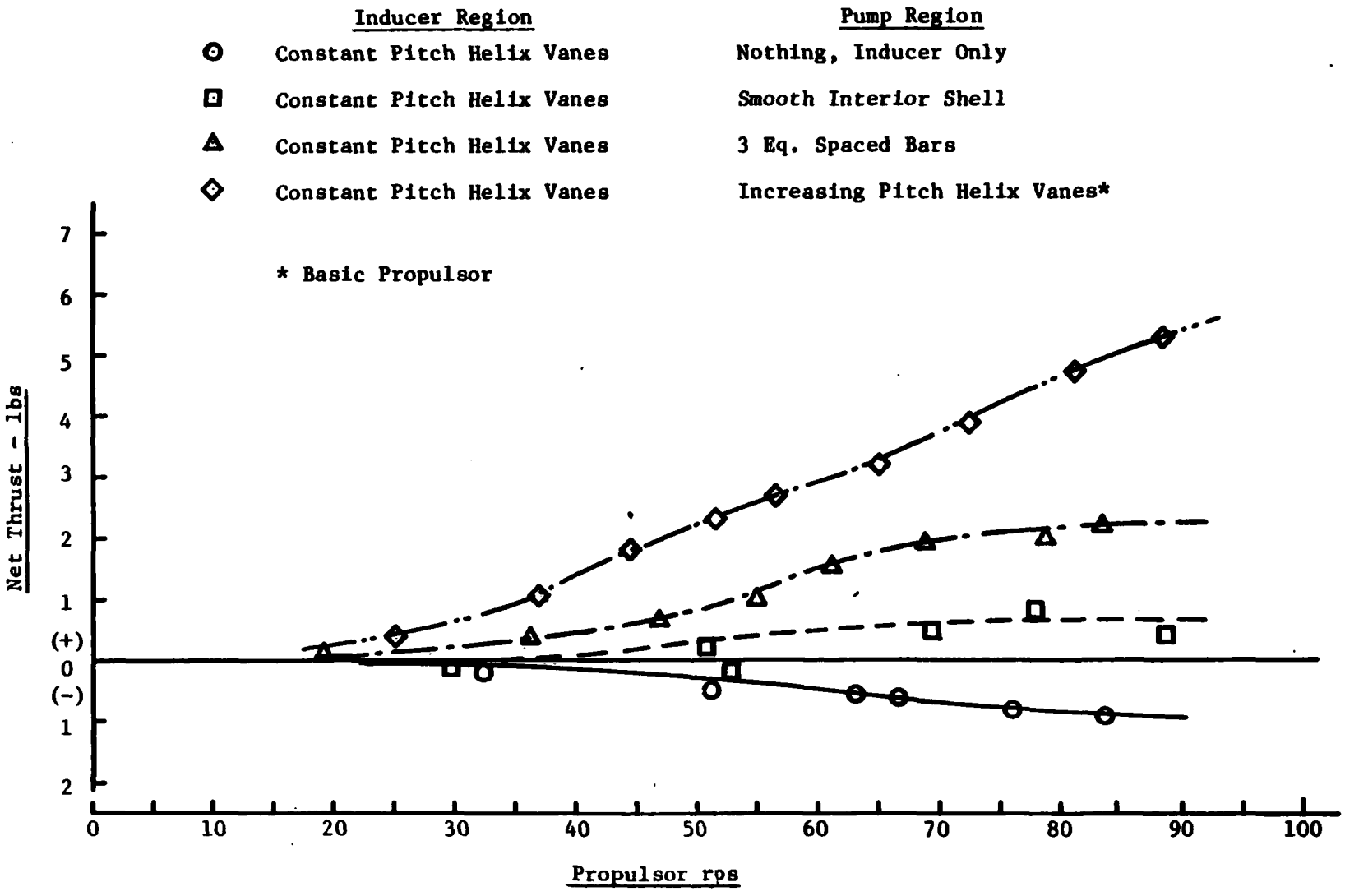

Figure 15 Thrust Comparison: Various Propulsor Configurations - Bollard Condition

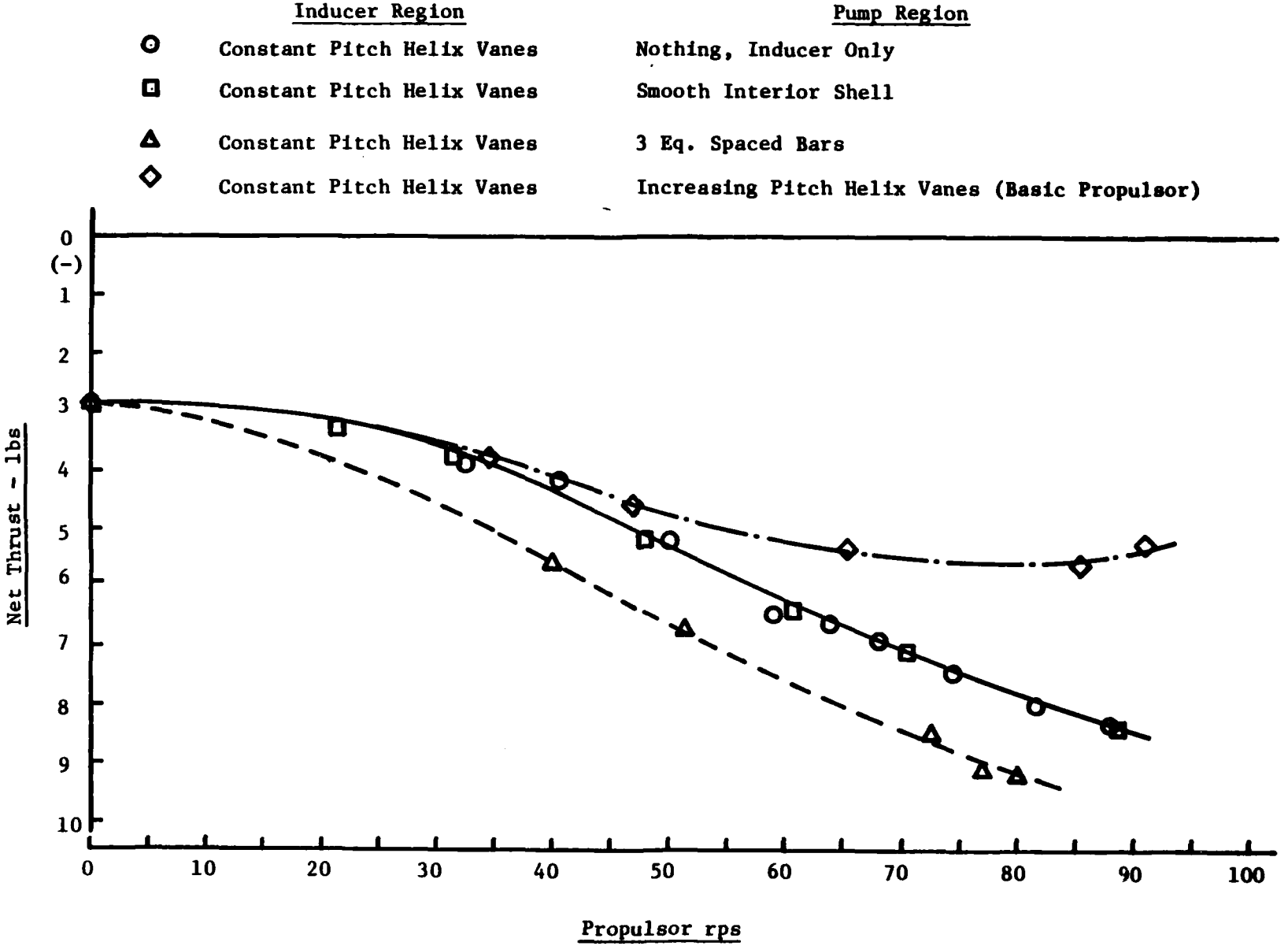

Figure 16 Comparison: Various Propulsor Configurations - Normalized Velocity ≈ 9.3 fps

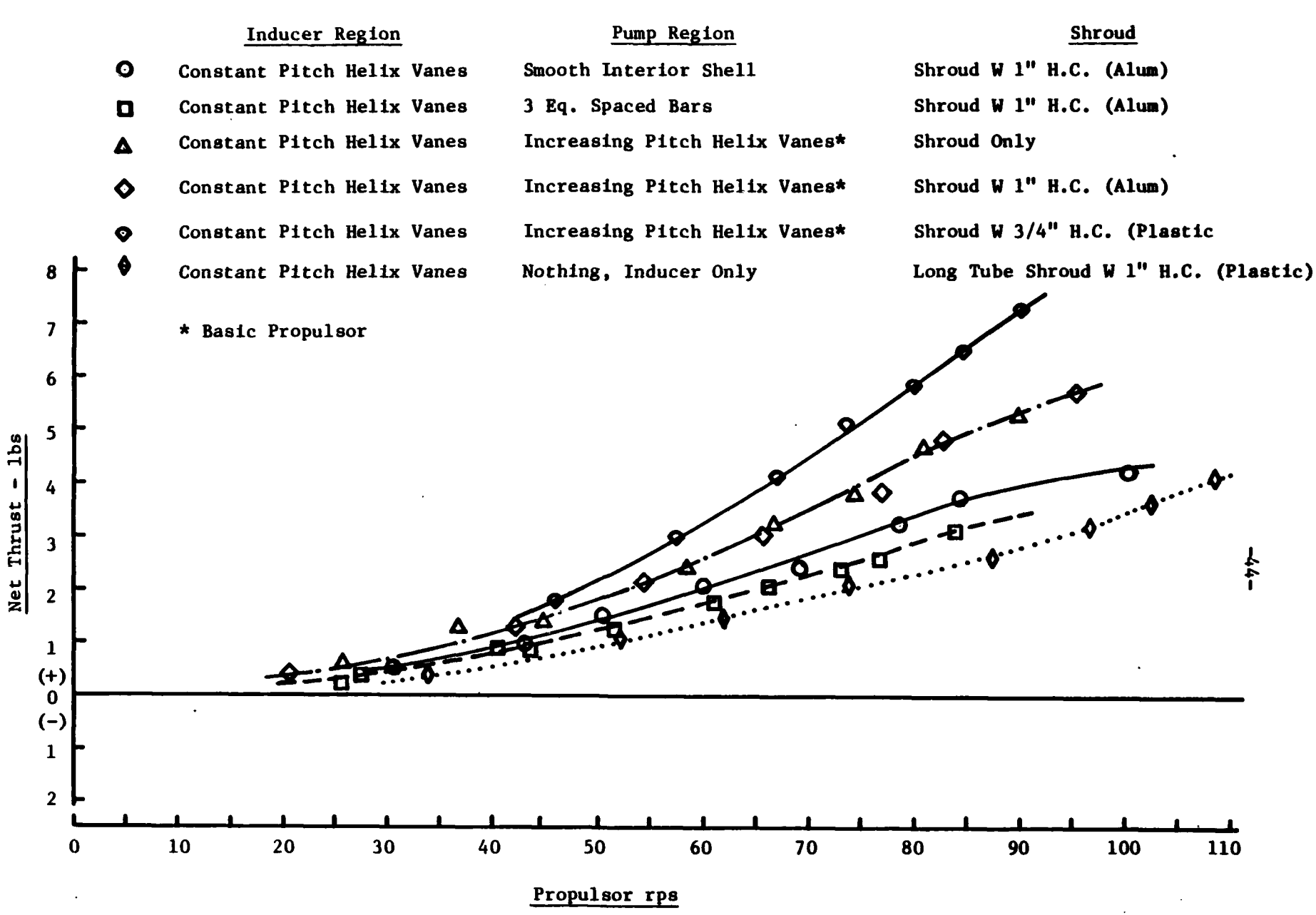

Figure 17 Comparison: Various Propulsor Configurations With Shroud - Bollard Conditions

	Inducer Region	Pump Region	Shroud
○	Constant Pitch Helix Vanes	Smooth Interior Shell	W 1" Alum Honeycomb
□	Constant Pitch Helix Vanes	3 Eq. Spaced Bars	W 1" Alum Honeycomb
△	Constant Pitch Helix Vanes	Increasing Pitch Helix Vanes*	Alone - No Honeycomb
◇	Constant Pitch Helix Vanes	Increasing Pitch Helix Vanes*	W 1" Alum Honeycomb
◈	Constant Pitch Helix Vanes	Increasing Pitch Helix Vanes*	W 3/4" Plastic Honeycomb
◆	Constant Pitch Helix Vanes	Nothing, Inducer Only	Long Tube W 1" Plastic H.C.

* Basic Propulsor

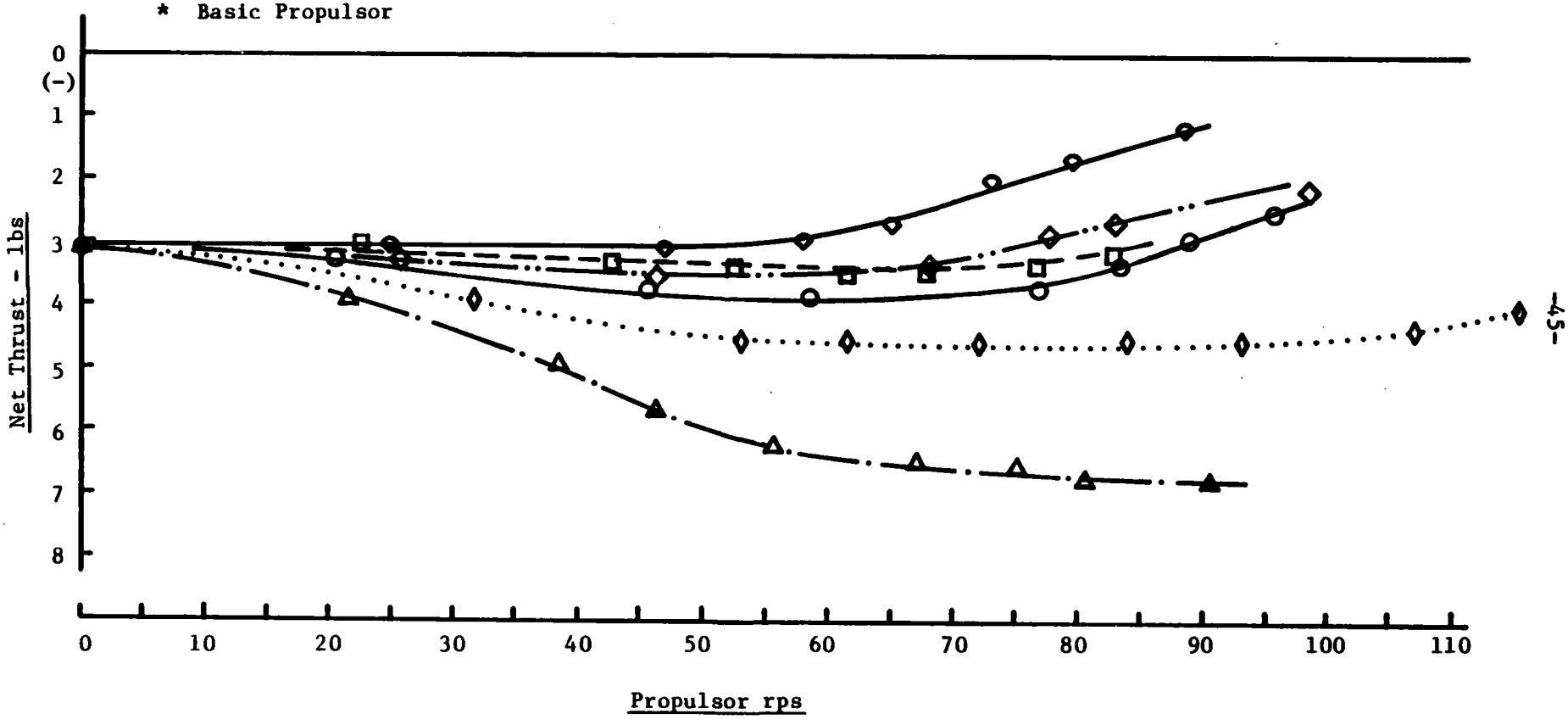

Figure 18 Comparison: Various Propulsor Configurations with Shroud - Normalized Velocity = 9.3 fps

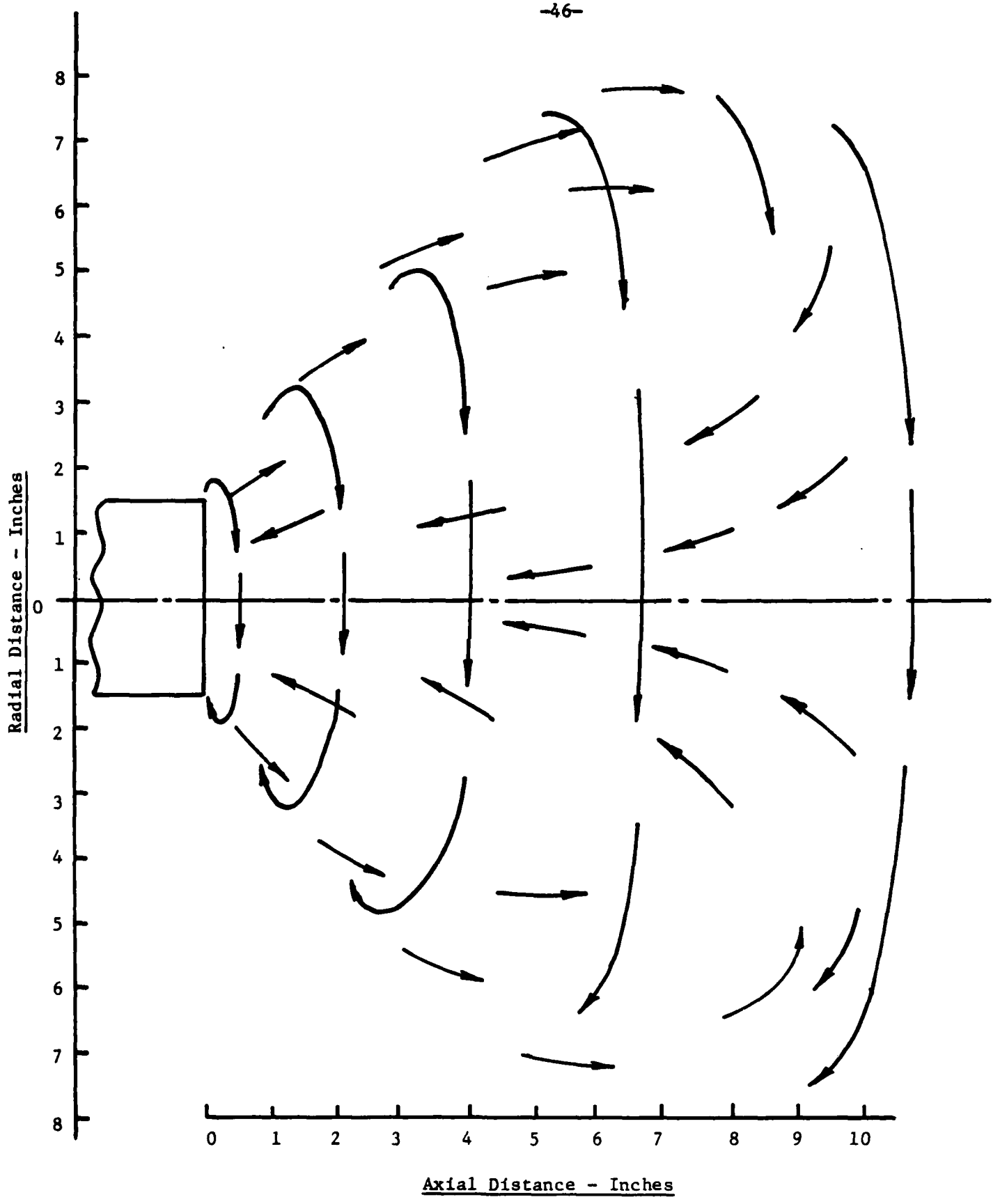

Figure 19 Flow Patterns: Basic Propulsor, Bollard Condition

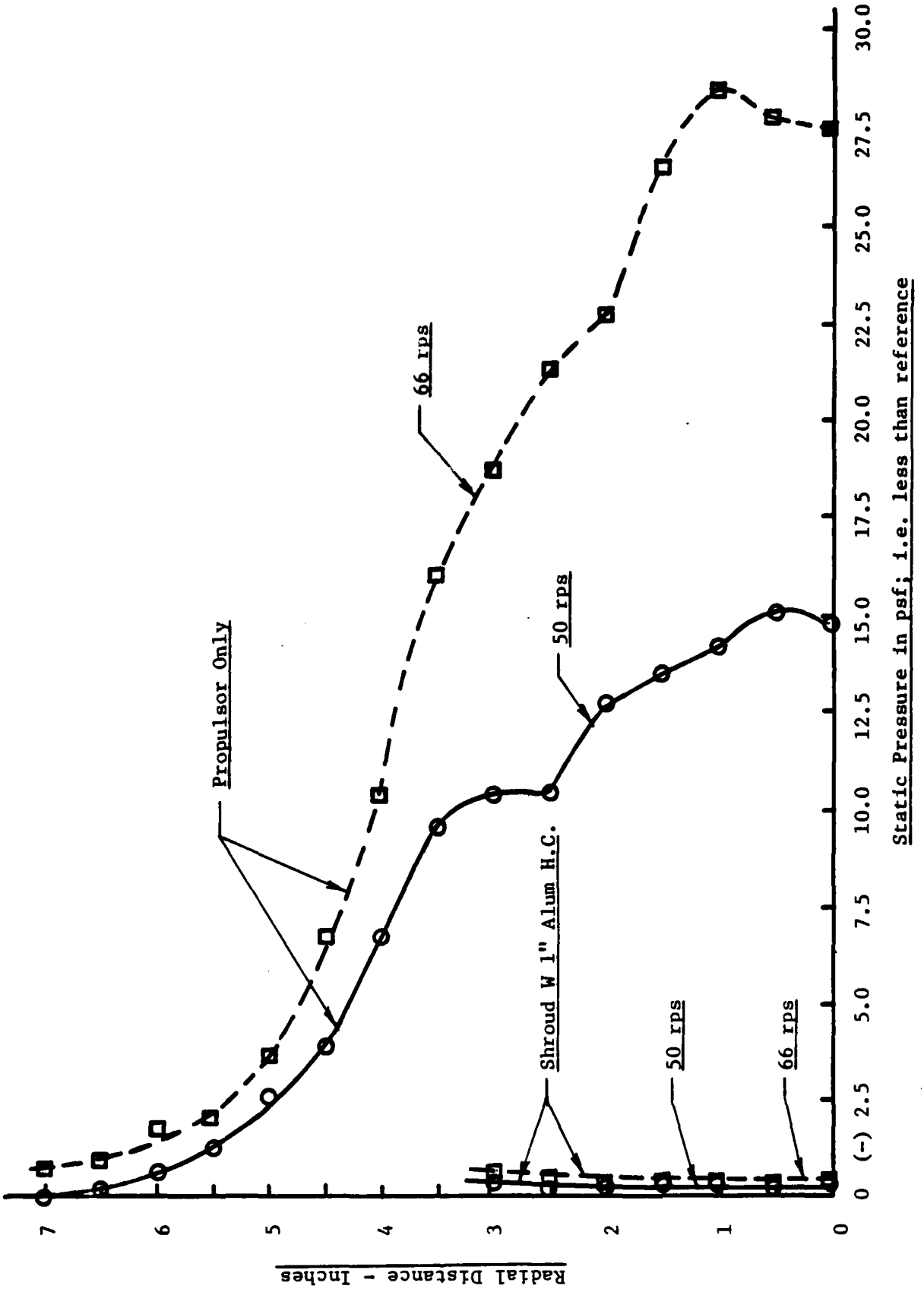

Figure 20 Static Pressure Surveys: Basic Propulsor - Bollard Condition

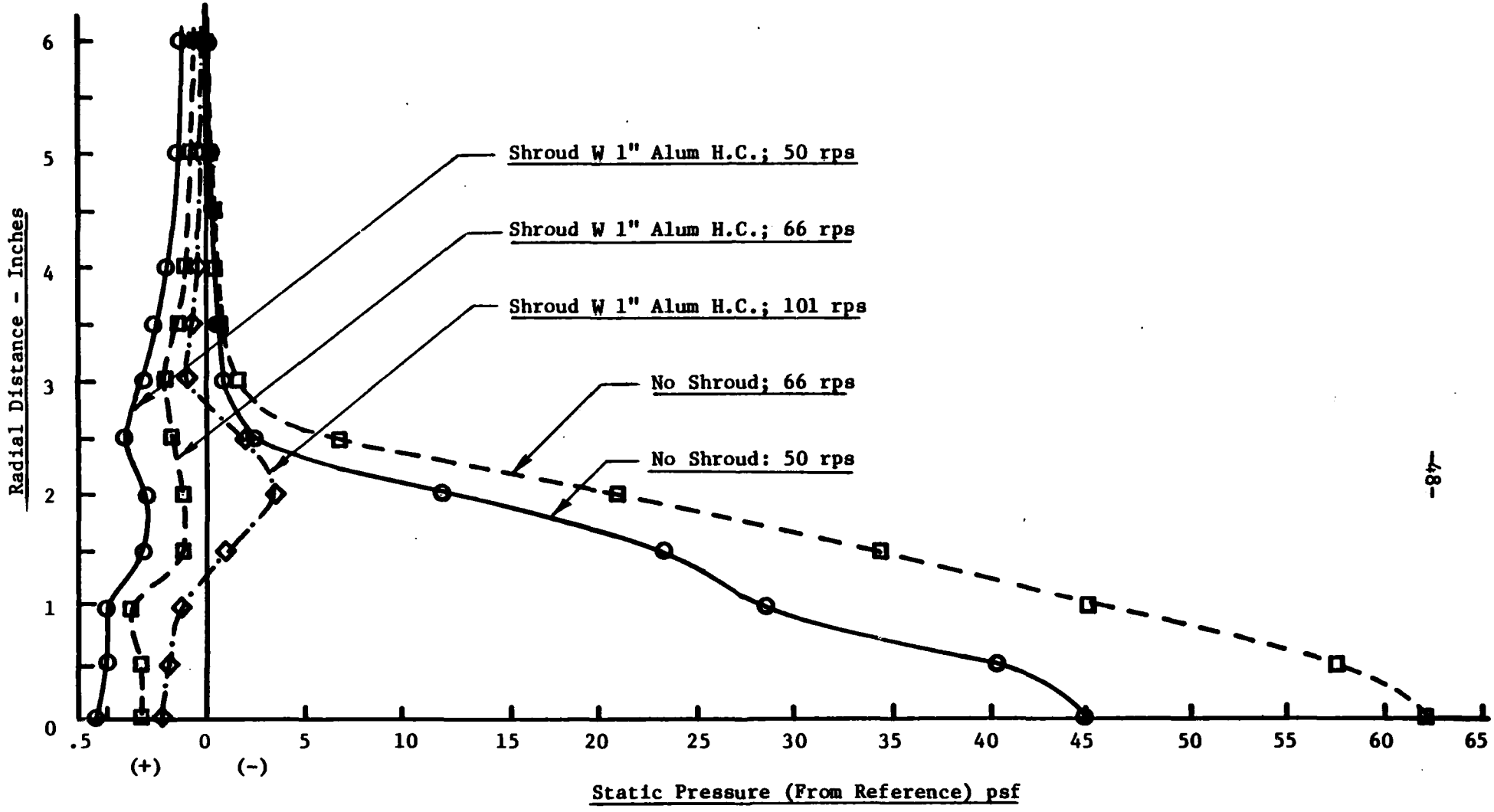

Figure 21 Static Pressure Surveys: Basic Propulsor - Noramlized Velocity = 9.3 fps

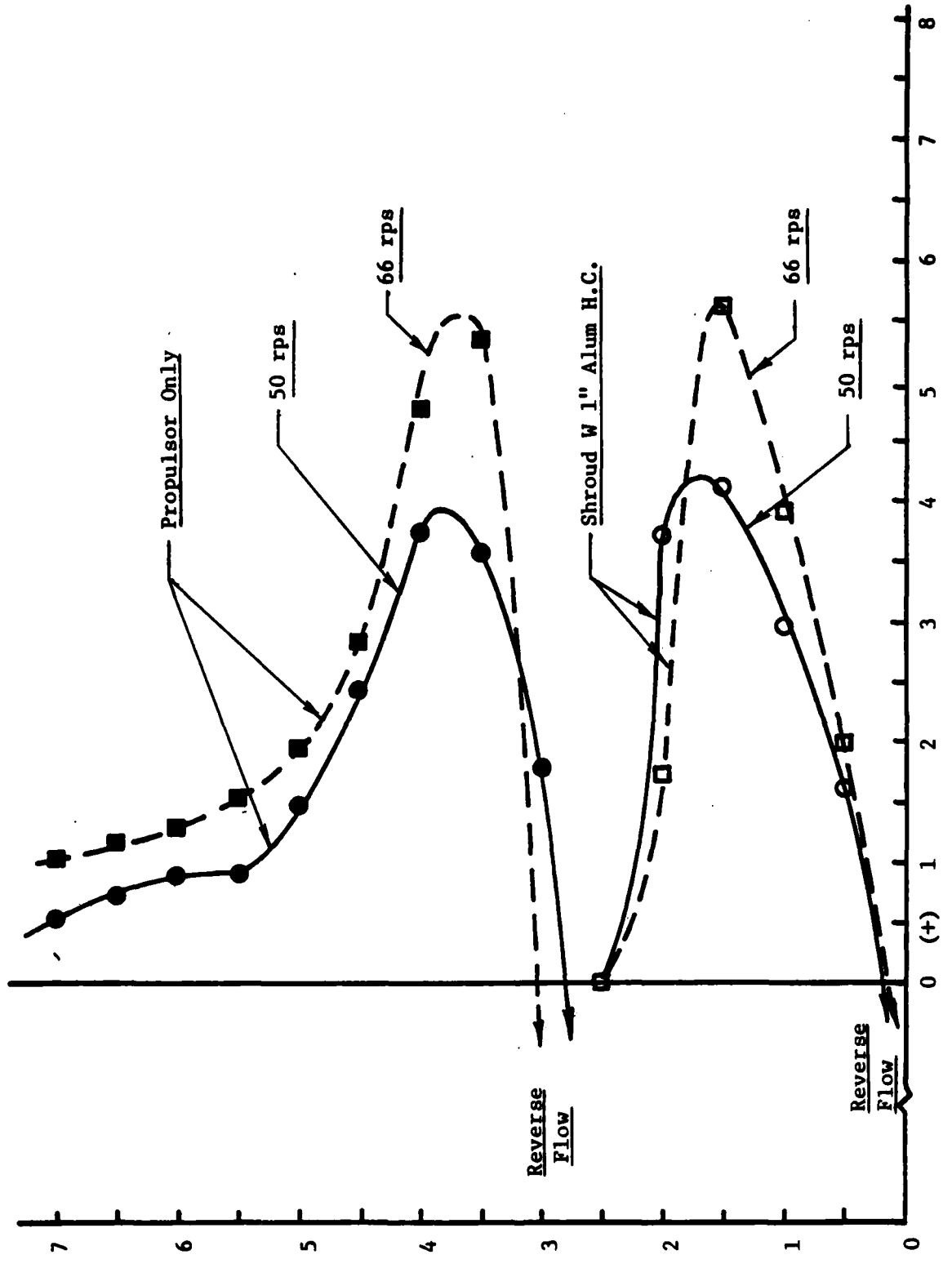

Figure 22 Axial Velocity Surveys: Basic Propulsor - Bollard Condition

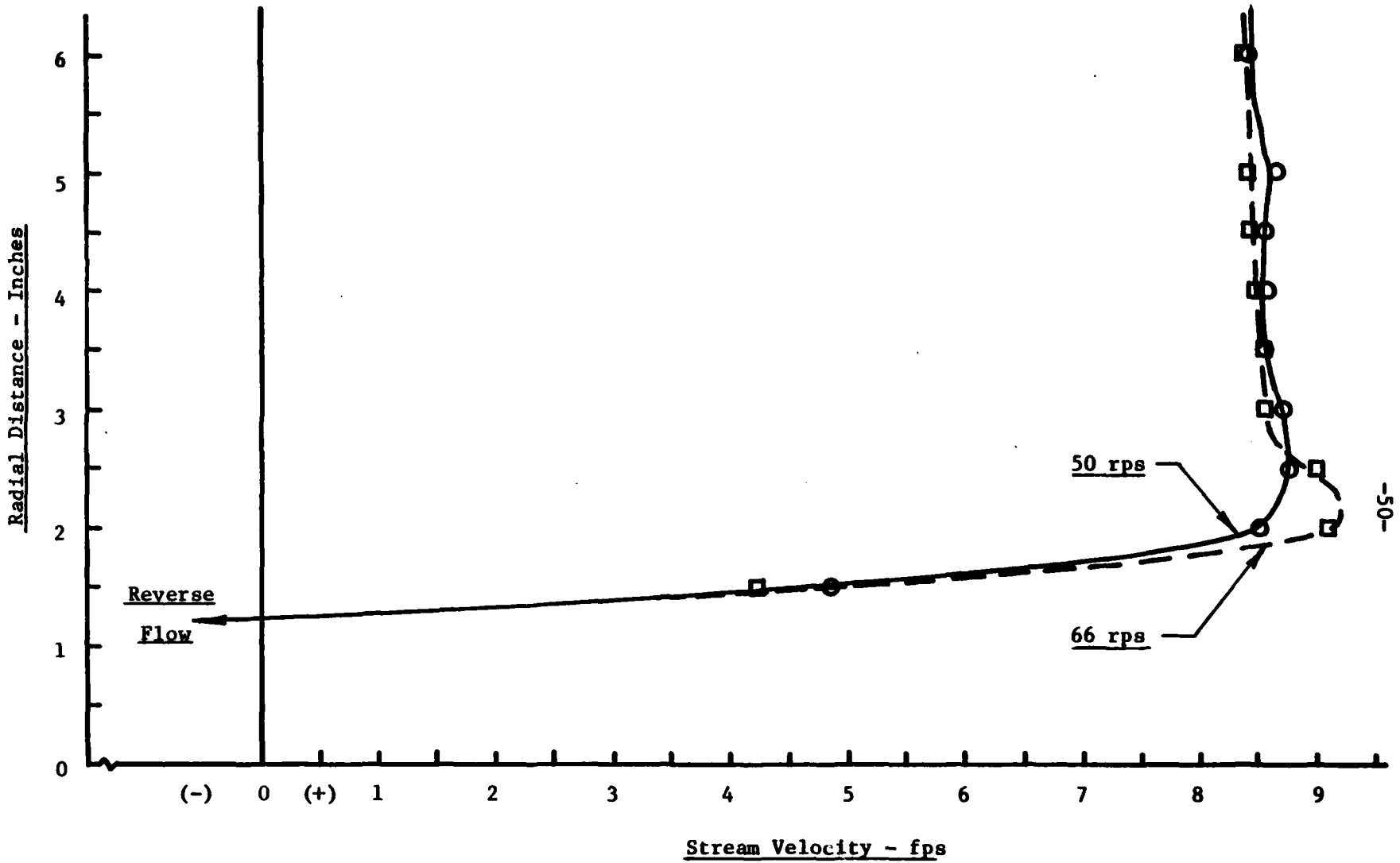

Figure 23 Axial Velocity Surveys: Basic Propulsor, No Shroud, With Free Stream Velocity

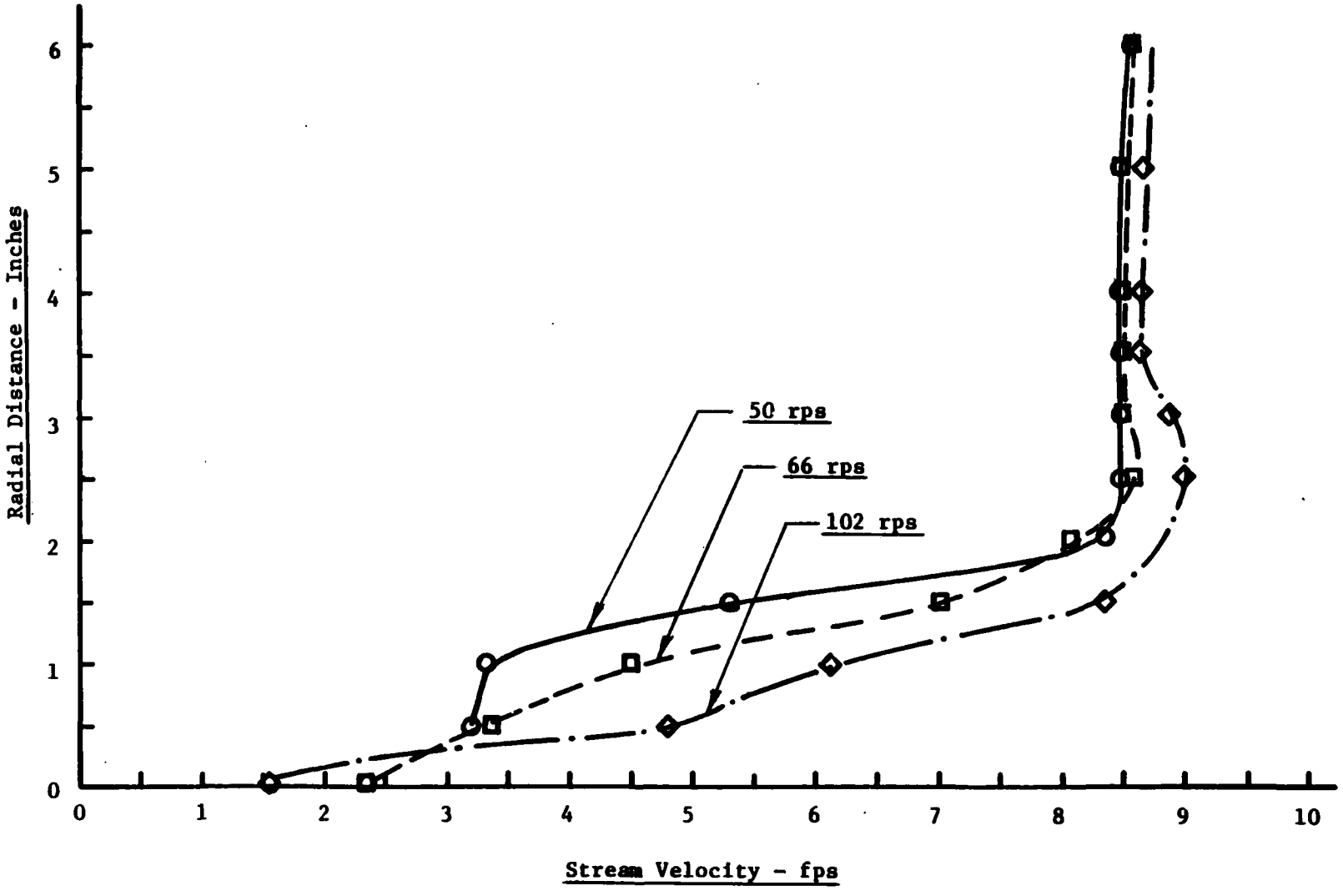

Figure 24 Axial Velocity Surveys: Basic Propulsor, Shroud W 1-Inch Alum Honeycomb, with Free Stream Velocity

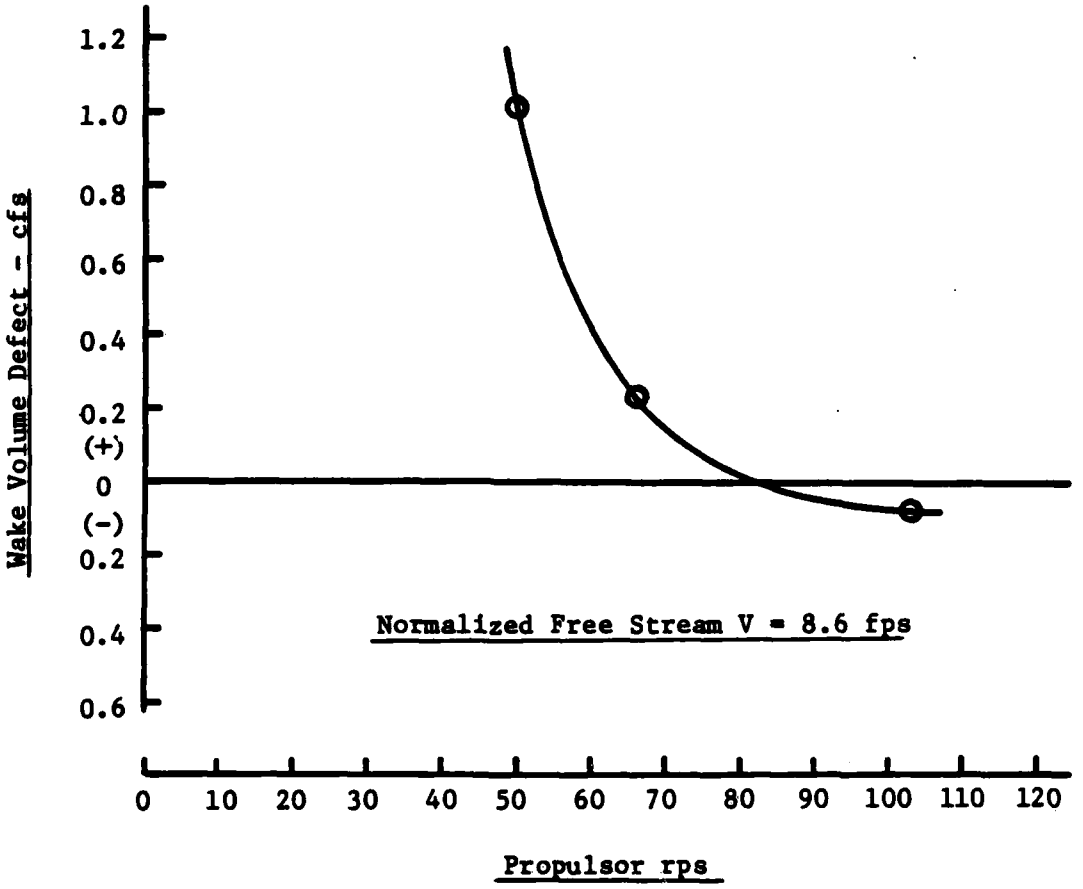

Figure 25 Wake Volume Defect: Basic Propulsor, Shroud With 1-Inch Alum Honeycomb

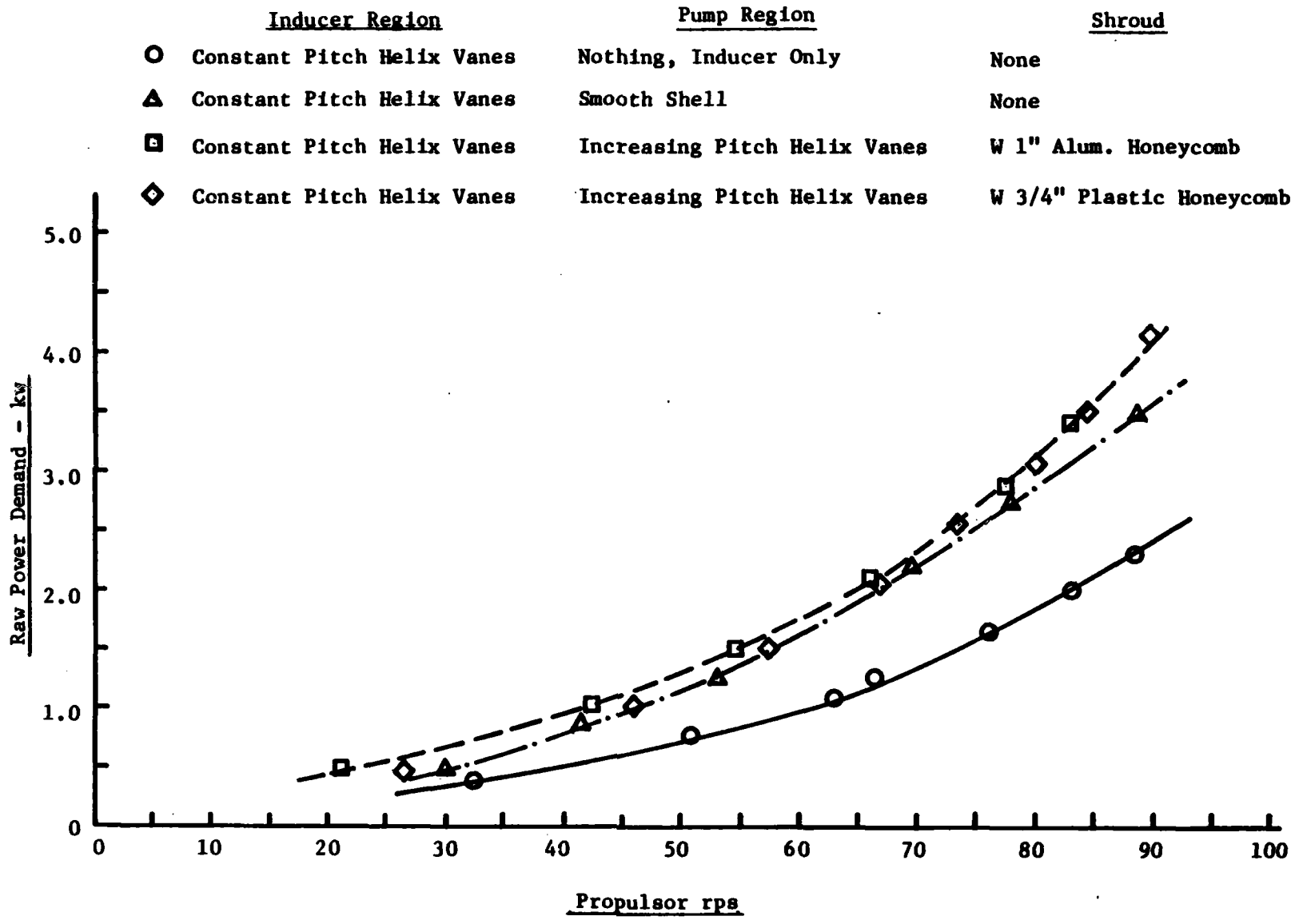

Figure 26 Raw Power Demand Comparion: Various Propulsor Configurations - Bollard Condition

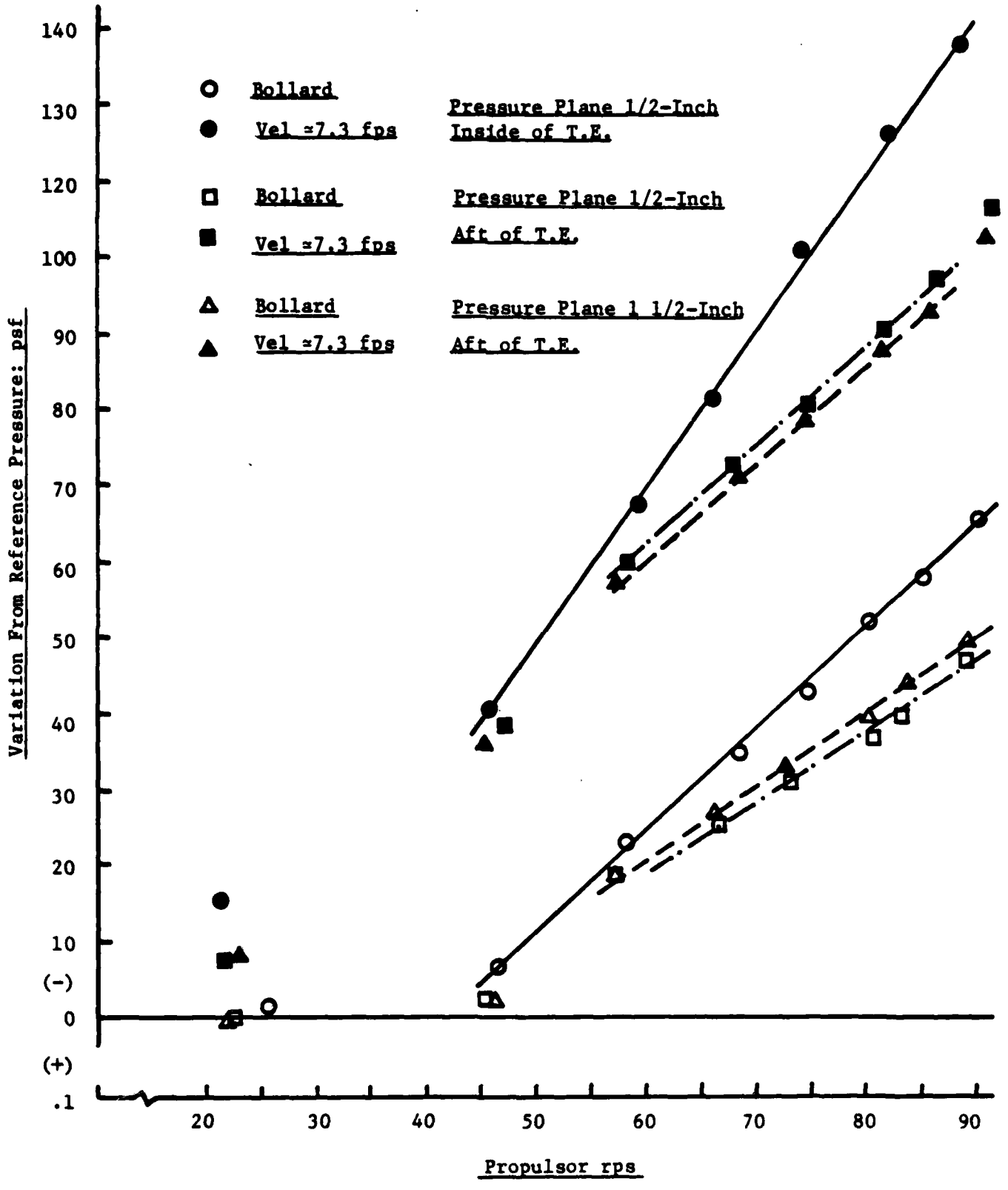

Figure 27 ℄ Core Pressures: Basic Propulsor, No Shroud

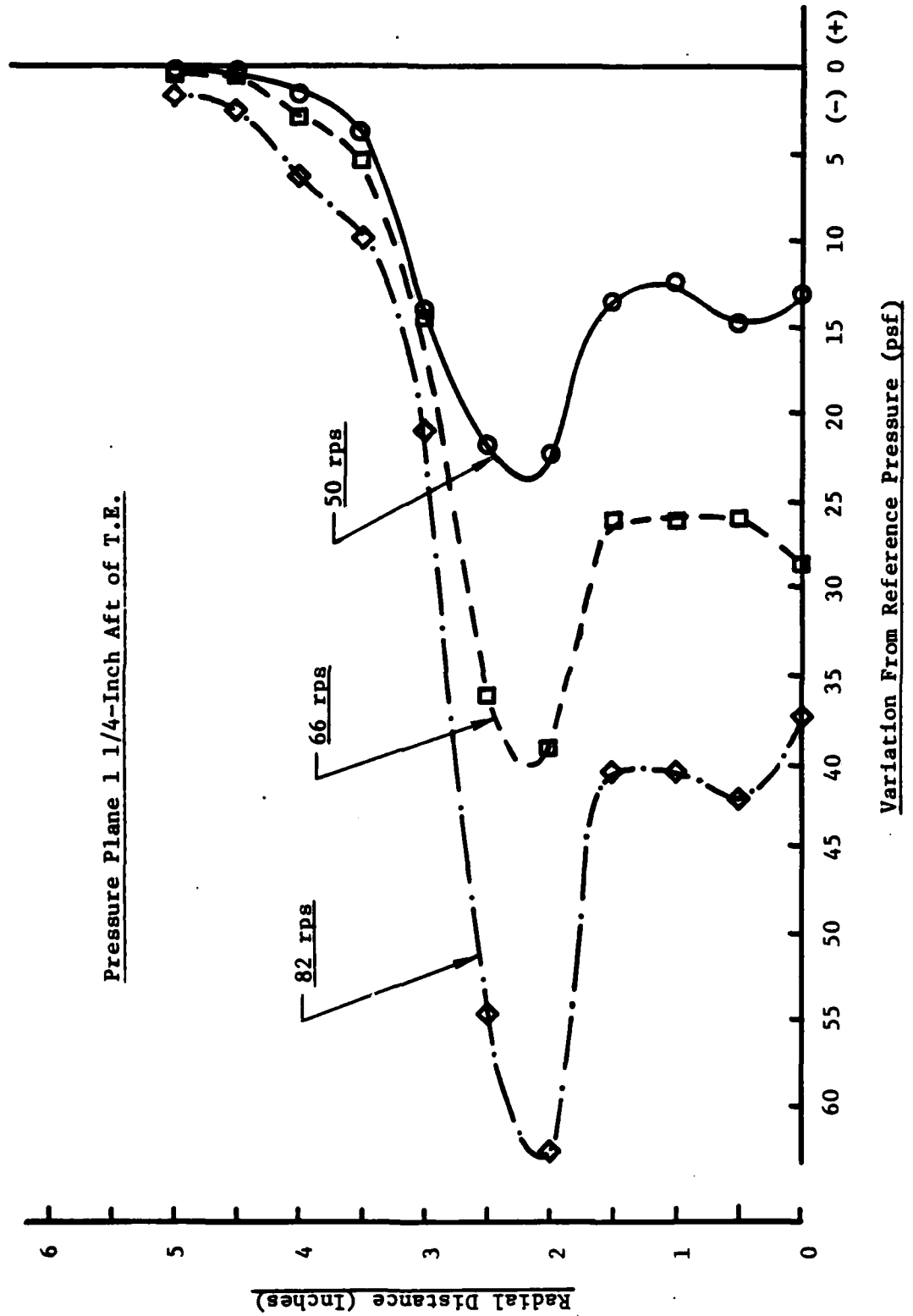

Figure 28 Static Pressures: Basic Propulsor, No Shroud

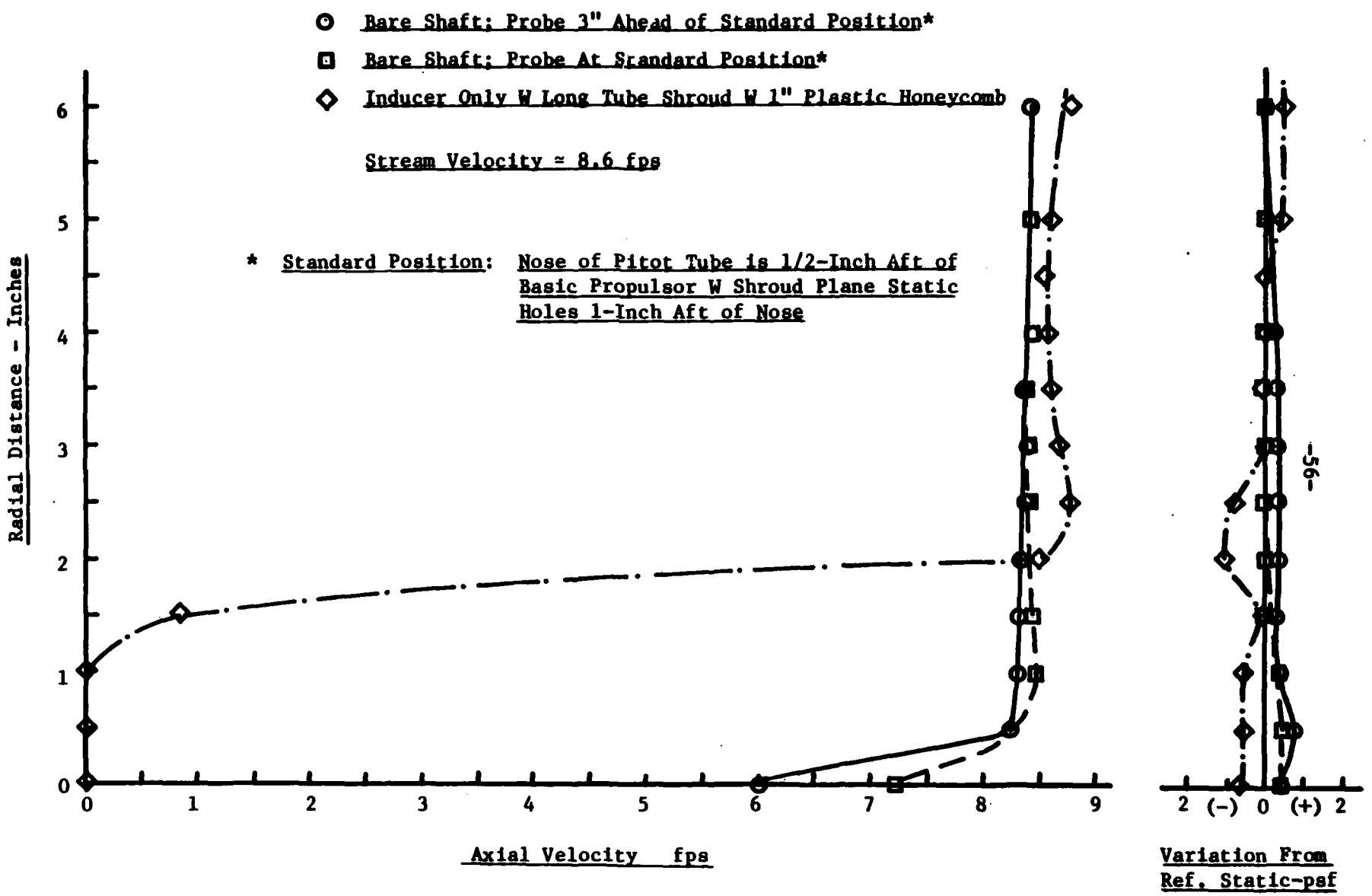

Figure 29 Velocity and Static Pressure Surveys

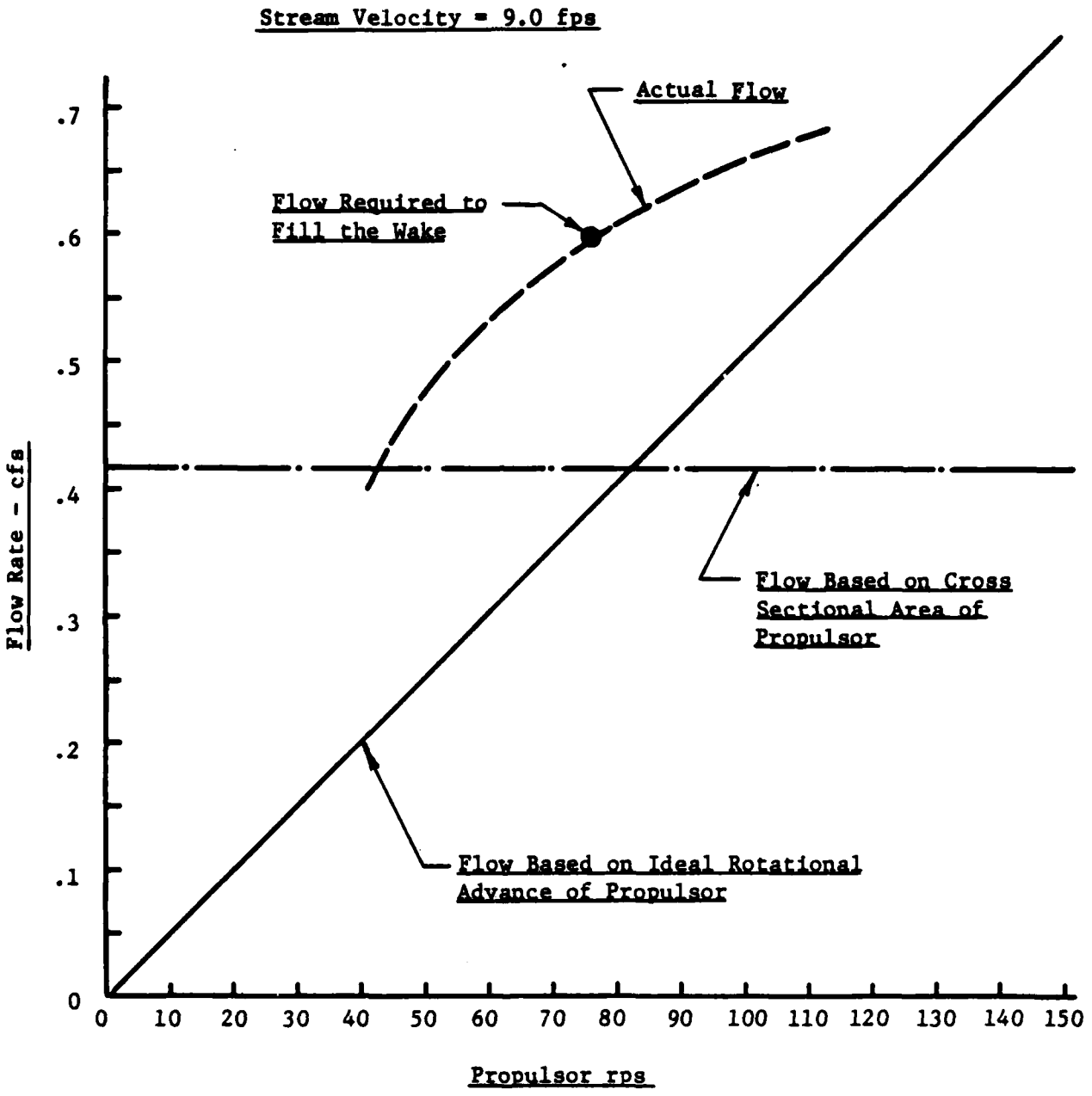

Figure 30 Comparison of Various Volume Flows: Basic Propulsor and Shroud W 1-Inch Alum Honeycomb

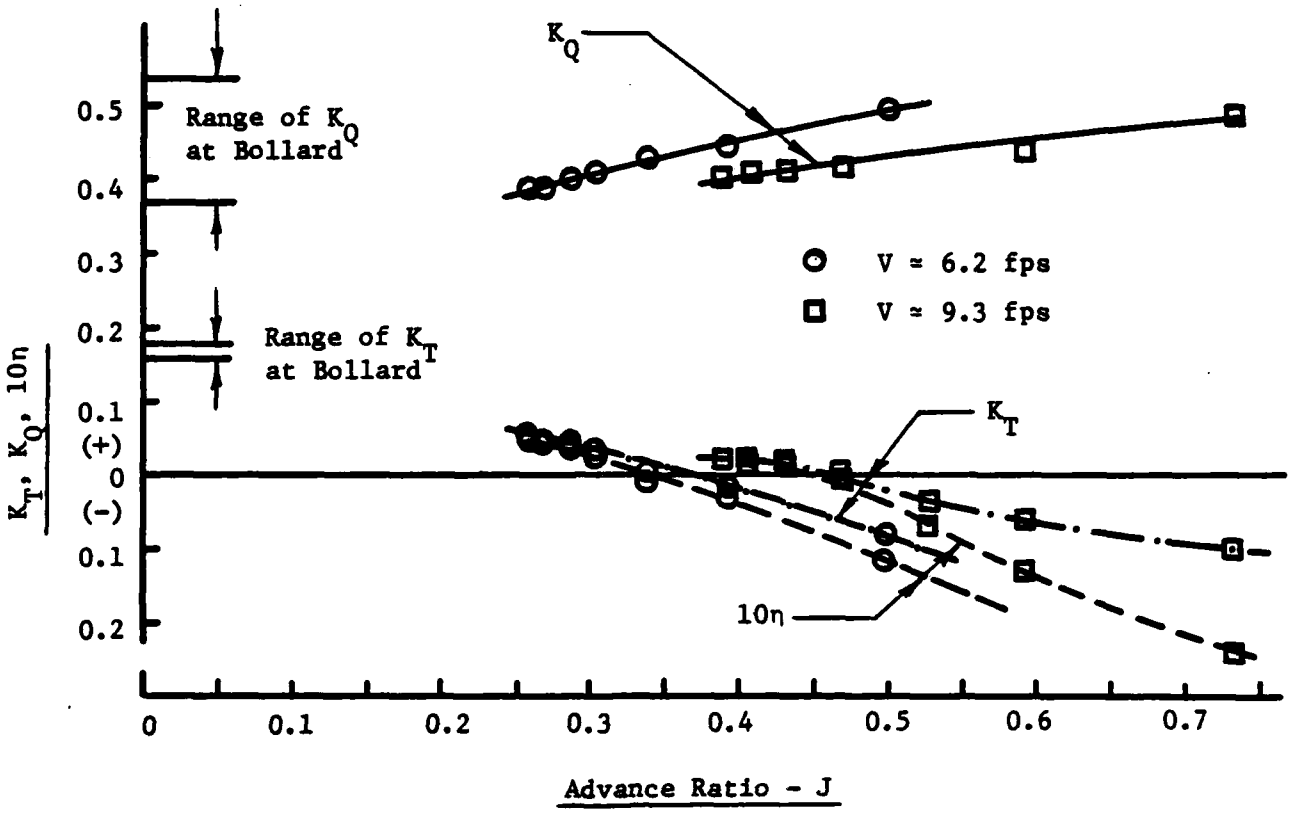

Figure 31 K_T, K_Q, η vs J: Basic Propulsor and Shroud W 3/4-Inch Plastic Honeycomb

DISTRIBUTION LIST

Entry Block 14, CDRL	Addressee	Activity Code
NAVSEA 63R-31	Commander Naval Sea Systems Command Department of the Navy Washington, D. C. 20362 Attn: Code 63R-31	N00024
NAVSEA 63R	Commander Naval Sea Systems Command Department of the Navy Washington, D. C. 20362 Attn: Code 63R	N00024
NAVSEA 63R-3	Commander Naval Sea Systems Command Department of the Navy Washington, D. C. 20362 Attn: Code 63R-3	N00024
NAVSEA PMS-408	Commander Naval Sea Systems Command Department of the Navy Washington, D. C. 20362 Attn: PMS-408	N00024
NAVSEA PMS-406	Commander Naval Sea Systems Command Department of the Navy Washington, D. C. 20362 Attn: PMS-406	N00024
DDC (2 Copies)	Defense Documentation Center Defense Services Administration Cameron Station, Building 5 5010 Duke Street Alexandria, Virginia 22314	S47031

DISTRIBUTION LIST (Continued)

Entry Block 14, CDRL	Addressee	Activity Code
NUSC	Commanding Officer Naval Underwater Systems Center Newport, Rhode Island 02840 Attn: Code 363	N91753
NUSC	Commanding Officer Naval Underwater Systems Center Newport, Rhode Island 02840 Attn: Code 36301	N91753
NOSC (2 copies)	Commander Naval Ocean Systems Center San Diego, CA 92152 Attn: Code 6342	N66001
ARL/PSU	Applied Research Laboratories The Pennsylvania State University P.O. Box 30 State College, PA 16801 Attn: Dr. Henderson	
ARL/PSU	Applied Research Laboratories The Pennsylvania State University P.O. Box 30 State College, PA 16801 Attn: Mr. Gearhart	
DTNSRDC	Commander David Taylor Naval Ship Research and Development Center Bethesda, MD 20034	N00167
AFLA (2 Copies)	A. F. Lehman Associates Incorporated P.O. Box 27 Centerport, New York 11721 Attn: A. F. Lehman	

DISTRIBUTION LIST (Continued)

Entry Block 14, CDRL	Addressee	Activity Code
ONR	Dr. Robert E. Whitehead Mechanics Division, ONR 800 North Quincy Street Arlington, Virginia 22217	
NAVSEA	Mr. William Sandberg, 32134 Hydromechanics Technology Section NAVSEA Headquarters NC-3 Washington, D. C. 20362	32134
NAVSEA	Mr. Frank Welling Director, Propulsion Systems Analysis Division NAVSEA Headquarters NC-4 Washington, D. C. 20362	
DTNSRDC	Mr. William Morgan Head, Ship Performance Department DTNSRDC Bethesda, Maryland 20034	
DTNSRDC	Dr. Justin McCarthy Head, Naval Hydromechanics Division DTNSRDC Bethesda, Maryland 20034	
NAVSEA	Mr. Raymoned Grady 63Y312 NAVSEA Headquarters NC-2 Washington, D. C. 20362	634312


4-8
DT